PARAMETER IDENTIFICATION PROBLEM IN THE HODGKIN-HUXLEY MODEL

JEMY A. MANDUJANO VALLE, ALEXANDRE L. MADUREIRA

ABSTRACT. The Hodgkin-Huxley (H–H) landmark model is described by a system of four nonlinear differential equations which describes how action potentials in neurons are initiated and propagated. However, obtaining some of the parameters of the model requires a tedious combination of experiments and data tuning. In this paper, we propose the use of a minimal error iteration method to estimate some of the parameters in the H–H model, given the measurements of membrane potential. We provide numerical results showing that the approach approximates well some of the model's parameters, using the measured voltage as data, even in the presence of noise.

1. INTRODUCTION.

The seminal work (Hodgkin and Huxley, 1952) uses voltage- and space-clamp techniques to obtain the parameters of the ionic channel model of the squid giant axon. In the space-clamped version of the H–H model, the membrane electrical potential $V : [0, T] \to \mathbb{R}$ solves

$$C_M \dot{V}(t) + I_{\text{ion}}(t) = I_{\text{ext}} \quad \text{in } (0, T], \tag{1}$$

where I_{ext} is the specific external current applied on the membrane, C_M is the specific membrane capacitance, V is the membrane potential, $\dot{V} = dV/dt$ is the rate of voltage change (dots denote time derivatives). The specific ionic current $I_{\text{ion}}(t) = I_{\text{Na}}(t) + I_{\text{K}}(t) + I_L(t)$ is the sum of potassium, sodium and leak currents satisfying:

$$I_{\text{K}} = G_{\text{K}}\ (V - V_{\text{K}}), \qquad I_{\text{Na}} = G_{\text{Na}}\ (V - V_{\text{Na}}), \qquad I_L = g_l\ (V - V_l), \tag{2}$$

where G_{K}, G_{Na} and g_l are the conductances for potassium, sodium and leakage channels, and the constants V_{K}, V_{Na} and V_l are Nernst equilibrium potentials. The conductances G_{Na} and G_{K} are functions that depend on time and the membrane potential, and the leakage conductance g_l is constant. The K^+ and Na^+ conductances behave as

$$G_{\text{K}}(V, t) = g_{\text{K}} n^a(t), \qquad G_{\text{Na}}(V, t) = g_{\text{Na}} m^b(t) h^c(t), \tag{3}$$

where g_{K} and g_{Na} are maximum conductances for K^+ and Na^+, and the exponents a, b and c are positive numbers modeling the number of gates in each channel. The functions m and h are the activation and inactivation variables for Na^+, and n is the activation function for K^+. These functions are unit-less gating variables taking values between 0 and 1. The kinetics of the potassium and sodium channels is governed by,

$$\dot{\mathcal{X}}(t) = \alpha_{\mathcal{X}}(V)(1 - \mathcal{X}(t)) - \beta_{\mathcal{X}}(V)\mathcal{X}(t) \quad \text{for } \mathcal{X} = m, n, h, \tag{4}$$

Date: September 30, 2021.

Key words and phrases. parameter identification, Hodgkin-Huxley Model, inverse problem, minimal error iteration method.

The authors acknowledge the financial support of the Brazilian funding agency CNPq; the second author also acknowledge the financial support funding agency FAPERJ, from the state of Rio de Janeiro.

where

$$\alpha_m(V) = \frac{(25-V)/10}{\exp((25-V)/10)-1}, \qquad \beta_m(V) = 4\exp(-V/18), \tag{5}$$

$$\alpha_n(V) = \frac{(10-V)/100}{\exp((10-V)/10)-1}, \qquad \beta_n(V) = 0.125\exp(-V/80), \tag{6}$$

$$\alpha_h(V) = 0.07\exp(-V/20), \qquad \beta_h(V) = \frac{1}{\exp((30-V)/10)+1}. \tag{7}$$

See (Hodgkin and Huxley, 1952; Ermentrout and Terman, 2010) and references therein for further details.

The initial condition for $\mathcal{X}$ is unknown, and we now describe a way to impose such value based on “steady values” for $\mathcal{X}$ (Bower and Beeman, 2012; Cox and Griffith, 2001; Hodgkin and Huxley, 1952). From Eq. (4), we have

$$\dot{\mathcal{X}}(t) = \frac{1}{\tau_{\mathcal{X}}(V)}\big(\mathcal{X}_\infty(V) - \mathcal{X}(t)\big), \tag{8}$$

where the steady-state solution and the time constant are, respectively,

$$\mathcal{X}_\infty(V) = \frac{\alpha_{\mathcal{X}}(V)}{\alpha_{\mathcal{X}}(V)+\beta_{\mathcal{X}}(V)} \qquad \text{and} \qquad \tau_{\mathcal{X}}(V) = \frac{1}{\alpha_{\mathcal{X}}(V)+\beta_{\mathcal{X}}(V)}.$$

In the experiments illustrated in (Hodgkin and Huxley, 1952, Figure 3), the membrane potential starts at its resting state V_0 and almost immediately jumps to a new clamp voltage V_c (Bower and Beeman, 2012, Page 40). Then, considering a constant membrane potential $V(t) = V_c$, we gather from Eq. (8) that

$$\dot{\mathcal{X}}(t) = \frac{1}{\tau_{\mathcal{X}}(V_c)}\big(\mathcal{X}_\infty(V_c) - \mathcal{X}(t)\big).$$

The solution to the previous equation is

$$\mathcal{X}(t) = \mathcal{X}_\infty(V_c) - (\mathcal{X}_\infty(V_c) - \mathcal{X}_\infty(V_0))\exp(-t/\tau_{\mathcal{X}}), \tag{9}$$

where we imposed $\mathcal{X}(0) = \mathcal{X}_\infty(V_0)$, for a given V_0. Note that $\mathcal{X} \to \mathcal{X}_\infty$ as $t \to \infty$. From the above, we have

$$\mathcal{X}(0) = \mathcal{X}_\infty(V_0) = \alpha_{\mathcal{X}}(V_0)/(\alpha_{\mathcal{X}}(V_0)+\beta_{\mathcal{X}}(V_0)) \quad \text{for} \quad \mathcal{X} = m, n, h. \tag{10}$$

We use the above approximation to fix the initial conditions of m, n, h.

Eqs. (1-10) yield the system of ordinary differential equations (ODEs):

$$\begin{cases} C_M\dot{V} + g_{\text{K}}n^a(V - V_{\text{K}}) + g_{\text{Na}}m^bh^c(V - V_{\text{Na}}) + g_l(V - V_l) = I_{\text{ext}} \quad \text{for } t \in (0,T], \\ \dot{\mathcal{X}} = (1-\mathcal{X})\alpha_{\mathcal{X}}(V) - \mathcal{X}\beta_{\mathcal{X}}(V) \quad \text{for } t \in (0,T], \\ V(0) = V_0, \qquad \mathcal{X}(0) = \mathcal{X}_\infty(V_0), \end{cases} \tag{11}$$

for $\mathcal{X} = m, n, h$, and C_M, I_{ext}, V_{K}, V_{Na} and V_l are known. Also, Eq. (10) defines the initial conditions for m, n and h. The units of the parameters are as in Table 1.

Using experimental data from the squid neuron, Hodgkin and Huxley obtained the parameters $a = 4$, $b = 3$ and $c = 1$. Note, however, that other models produce different parameters, e.g. for $I_{\text{Na},p} + I_{\text{K}}$-model $(a,b,c) = (1,1,0)$, for $I_{\text{Na},t}$-model $(a,b,c) = (0,3,1)$ and for I_A-model $(a,b,c) = (0,1,1)$; see (Izhikevich, 2007).

Parameters	**Units**	**Units name**
C_M	$\mu F/cm^2$	microfarad per square centimeter
V	mV	millivolt
$\dot{V}$	V/s	volts per second
I_{ext}, I_{ion}	$\mu A/cm^2$	microampere per square centimeter
g_{K}, g_{Na}, g_l	mS/cm^2	millisiemens per square centimeter
V_{K}, V_{Na}, V_l	mV	millivolt
t	ms	milliseconds

TABLE 1. Units of the parameters; see (Hodgkin and Huxley, 1952, Table 3).

Parameter determination is an important issue in neuroscience. In a previous paper (Valle et al., 2020), the authors determine conductances with nonuniform distribution in the equation of the cable with and without branches, using the minimal error iterative method. See also (Avdonin and Bell, 2013, 2015; Bell and Craciun, 2005; Tadi et al., 2002), for identification of parameters in the cable equation.

Parameter identification for the FitzHugh-Nagumo model is considered in (Cox and Wagner, 2004; Cox and Ji, 2001), where the authors determine the nonlinear conductance among other parameters. Also, (He and Keyes, 2007) study the reactive coefficient identification problem for the the same system, using Newton-Krylov iterations.

In the following, we describe the different studies that estimated parameters in the H–H model. Given the conductance from a clamp-tension experiment, (Wang and Beaumont, 2004; Willms et al., 1999) estimate the steady-state constants m_∞, n_∞, h_∞, the time constants τ_m, τ_n,τ_h, and kinetic properties. The identifiability analysis of the H-H model parameters is discussed in (Csercsik et al., 2012; Walch and Eisenberg, 2016), where the authors show that is possible to estimate the model parameters from voltage-clamp data.

In (Cox and Griffith, 2001), the authors consider a linearized model to determine the resistivity, membrane capacitance, and maximal conductances in dendritic neurons with the moment method. The constant parameters of an ionic channel are estimated simultaneously in (Buhry et al., 2011, 2012) using the differential evolution algorithm. Also, (Daly et al., 2015) investigate the use of approximate Bayesian computation to infer parameters in the sodium and potassium channels. For most of the above references, it is not clear how to extend the methods to compute the exponents modeling the number of gates in each channel, or to consider spatially dependent problems for spatially heterogeneous neurons. Although not explored in the present work, we believe that methods that deal with spatial properties will become more relevant in the near future, in particular in view of more advance imaging techniques (Casale et al., 2015; Grinvald and Hildesheim, 2004). And the present method can be, in principle, extended to spacial problems (Valle et al., 2020).

We propose an iterative method to determine unknown parameters in the H–H system (11), given the measurements of membrane potential (data with noise). The method is an alternative to the classical estimation methods associated with voltage clamp measurements. In this work, we present two different inverse problems. The first problem is to estimate maximum conductances (g_{K}, g_{Na} and g_l), while the second problem is to determine exponents of the activation and inactivation variables (a, b, and c). Our approach can also recover functions with non-uniform distribution (Valle et al., 2020).

Inverse problems are said to be *ill-posed*, in the sense of (Hadamard, 2014). A problem is well-posed if there is a unique solution, which has a continuous dependence on the input data (stability). Here we admit the existence of a single solution to the problem. However, stability is not guaranteed. Stability is necessary if we want to ensure that small variations in the data lead to small changes in the solution. Problems of instability can be controlled by regularization methods, in particular the minimal error iterative scheme (Binder et al., 1996; Chapko and Kügler, 2004; Hanke et al., 1995; Neubauer, 2000).

There are several iterative regularization methods; see (Benning and Burger, 2018) for a thorough review on the subject. One instance is the minimal error method, that we employ here. Methods like these have the advantage of avoiding big matrix-invertions (as in Newton-like methods), although they might require more iterations to converge; see (Nayak, 2021). We remark that the minimal error method is an improvement on the classical Landweber and modified Landweber methods, that might not even converge at all in general, see Appendix C.

The four dimensional H-H model presents hurdles that simpler models try to overcome by bringing down its dimension. Well-known examples include the FitzHugh-Nagumo model, the Krinsky-Kokoz model and the Morris-Lecar model (FitzHugh, 1961; Krinskiĭ and Kokoz, 1973; Morris and Lecar, 1981). These mathematical formulations also describe how action potentials, in a neuron, are initiated and propagated. Moreover, since recording the activity of a single neuron is far from being trivial, recording a population of neurons is more realistic. The mean field models or population models, describe the temporal evolution of the electrical activity of neuronal populations, these formulations are coupled ordinary differential equations (Bojak et al., 2010; Buzsáki et al., 2012; Liley et al., 2001).

All the above models involve varying number of hard to compute unknown parameters. We believe that our scheme is general enough to estimate unknown parameters of those models even under the presence of measurements errors.

We now describe the contents of the present paper briefly. Section 2 presents our inverse problems for the H–H model along with some theoretical results, and in Section 3 we show numerical results to describe the effectiveness of our strategy. Finally, we include in the Appendices some more technical arguments.

2. Inverse Problem in the H–H model

In what follows, we describe an abstract formulation of the minimal error method; see (Kaltenbacher et al., 2008).

Consider ODE (11), and let $\boldsymbol{x} = (g_{\mathrm{K}}, g_{\mathrm{Na}}, g_l) \in \mathbb{R}^3$ or $\boldsymbol{x} = (a, b, c) \in \mathbb{R}^3$. Consider also the set of square integrable functions $L^2[0, T]$, and the nonlinear operator

$$F : \mathbb{R}^3 \to L^2[0, T], \tag{12}$$

defined by $F(\boldsymbol{x}) = V$, where V solves the system of ODEs (11). In practical terms, the "real" data V are obtained by noisy measurements denoted by V^δ, of the which we assume to know the noise level δ, where

$$\|V - V^\delta\|_{L^2[0,T]} := \sqrt{\int_0^T (V(t) - V^\delta(t))^2\, dt} \leq \delta. \tag{13}$$

We assume that the equation $F(\boldsymbol{x}) = V$ has a unique solution x_*, and denote $V^\delta = F(\boldsymbol{x}^\delta)$.

To obtain an approximation of $\boldsymbol{x}$, given V^δ, we used the minimal error iteration

$$\boldsymbol{x}^{k+1,\delta} = \boldsymbol{x}^{k,\delta} + w^{k,\delta} F'(\boldsymbol{x}^{k,\delta})^*(V^\delta - V^{k,\delta}), \tag{14}$$

where $F'(\boldsymbol{x}^{k,\delta})$ is the Gateaux-derivative of F computed at $\boldsymbol{x}^{k,\delta}$, $F'(\boldsymbol{x}^{k,\delta})^*$ is its adjoint, and $V^{k,\delta} = F(\boldsymbol{x}^{k,\delta})$. We also define

$$w^{k,\delta} = \frac{\|V^\delta - V^{k,\delta}\|^2_{L^2[0,T]}}{\|F'(\boldsymbol{x}^{k,\delta})^*(V^\delta - V^{k,\delta})\|^2_{\mathbb{R}^3}},$$

where $\|\cdot\|_{\mathbb{R}^3}$ is the Euclidian norm.

The iteration (14) begins with a guess $\boldsymbol{x}^{1,\delta}$ and stops at the minimum $k_* = k(\delta, V^\delta)$, such that, for a given $\tau > 1$,

$$\|V^\delta - F(\boldsymbol{x}^{k_*,\delta})\|_{L^2[0,T]} = \|V^\delta - V^{k_*,\delta}\|_{L^2[0,T]} \leq \tau\delta. \tag{15}$$

It is possible to show that, under certain conditions, $\boldsymbol{x}^{k_*,\delta}$ converges to a solution of $F(\boldsymbol{x}) = V$ as $\delta \to 0$; see (Neubauer, 2018).

Remark 1. *The computation of the action of adjoint of the Gateaux-derivative of F is far from trivial, and has to be found in a case-by-case basis. That is done for the Gompertz model (Valle, 2020) and the linear cable equation (Valle et al., 2020). See also the supplementary material, where we compare the current approach with other methods.*

2.1. **Inverse Problem to obtain conductances in the H–H model.** The present goal is to estimate the maximum conductances $\boldsymbol{x} = \boldsymbol{g} = (g_{\mathrm{K}}, g_{\mathrm{Na}}, g_l)$ while assuming that (11) holds and that the exponents a, b, and c are known. From iteration (14), we have

$$\boldsymbol{g}^{k+1,\delta} = \boldsymbol{g}^{k,\delta} + w^{k,\delta} F'(\boldsymbol{g}^{k,\delta})^*(V^\delta - V^{k,\delta}), \tag{16}$$

where $\boldsymbol{g}^{k,\delta} = (g_{\mathrm{K}}^{k,\delta}, g_{\mathrm{Na}}^{k,\delta}, g_l^{k,\delta})$.

The action of the operator $F'(\boldsymbol{g}^{k,\delta})^*$ is non-trivial, and we describe it in the following theorem while postponing the proof for the appendix.

Theorem 2.1. *Assume that a, b, c, V_{Na} ,V_K, V_l, C_M, I_{ext}, V_0, m_0, n_0, h_0 and T are known data. Assume also that $\boldsymbol{g}^{k,\delta} = (g_K^{k,\delta}, g_{Na}^{k,\delta}, g_l^{k,\delta})$ are known, and that $V^\delta = F(\boldsymbol{g}^\delta)$ and $V^{k,\delta} = F(\boldsymbol{g}^{k,\delta})$. Then*

$$F'(\boldsymbol{g}^{k,\delta})^*(V^\delta - V^{k,\delta}) = \left(X_K^{k,\delta}, X_{Na}^{k,\delta}, X_l^{k,\delta}\right), \tag{17}$$

where

$$X_K^{k,\delta} = \int_0^T \left(n^{k,\delta}\right)^a (V^{k,\delta} - V_K) U^{k,\delta}\, dt, \tag{18}$$

$$X_{Na}^{k,\delta} = \int_0^T \left(m^{k,\delta}\right)^b \left(h^{k,\delta}\right)^c (V^{k,\delta} - V_{Na}) U^{k,\delta}\, dt, \tag{19}$$

$$X_l^{k,\delta} = \int_0^T (V^{k,\delta} - V_l) U^{k,\delta}\, dt. \tag{20}$$

The functions $m^{k,\delta}$, $n^{k,\delta}$, $h^{k,\delta}$ and $V^{k,\delta}$ solve,

$$
\begin{cases}
C_M\dot V^{k,\delta} + g_K^{k,\delta}\big(n^{k,\delta}\big)^a(V^{k,\delta}-V_K) + g_{Na}^{k,\delta}\big(m^{k,\delta}\big)^b\big(h^{k,\delta}\big)^c(V^{k,\delta}-V_{Na}) \\
\qquad + g_l^{k,\delta}(V^{k,\delta}-V_l) = I_{ext}, \\
\dot{\mathcal{X}}^{k,\delta} = (1-\mathcal{X}^{k,\delta})\alpha_{\mathcal{X}}(V^{k,\delta}) - \mathcal{X}^{k,\delta}\beta_{\mathcal{X}}(V^{k,\delta}) \quad \textit{for} \quad \mathcal{X}=m,n,h, \\
V^{k,\delta}(0)=V_0, \quad m^{k,\delta}(V_0,0)=m_0, \quad n^{k,\delta}(V_0,0)=n_0, \quad h^{k,\delta}(V_0,0)=h_0,
\end{cases}
\tag{21}
$$

and $\alpha_{\mathcal{X}}$, $\beta_{\mathcal{X}}$ are defined by (5-7). Finally, $U^{k,\delta}$ solves, given $m^{k,\delta}$, $n^{k,\delta}$, $h^{k,\delta}$ and $V^{k,\delta}$,

$$
\begin{cases}
C_M\dot U^{k,\delta} - \Big(g_K^{k,\delta}\big(n^{k,\delta}\big)^a + g_{Na}^{k,\delta}\big(m^{k,\delta}\big)^b\big(h^{k,\delta}\big)^c + g_l^{k,\delta}\Big)U^{k,\delta} \\
-[(1-m^{k,\delta})\alpha_m'(V^{k,\delta}) - m^{k,\delta}\beta_m'(V^{k,\delta})]P^{k,\delta} \\
-[(1-n^{k,\delta})\alpha_n'(V^{k,\delta}) - n^{k,\delta}\beta_n'(V^{k,\delta})]Q^{k,\delta} \\
-[(1-h^{k,\delta})\alpha_h'(V^{k,\delta}) - h^{k,\delta}\beta_h'(V^{k,\delta})]R^{k,\delta} = V^\delta - V^{k,\delta}, \\
\dot P^{k,\delta} - [\alpha_m(V^{k,\delta})+\beta_m(V^{k,\delta})]P^{k,\delta} = -bg_{Na}^{k,\delta}\big(m^{k,\delta}\big)^{b-1}\big(h^{k,\delta}\big)^c(V^{k,\delta}-V_{Na})U^{k,\delta}, \\
\dot Q^{k,\delta} - [\alpha_n(V^{k,\delta})+\beta_n(V^{k,\delta})]Q^{k,\delta} = -ag_K^{k,\delta}\big(n^{k,\delta}\big)^{a-1}(V^{k,\delta}-V_K)U^{k,\delta}, \\
\dot R^{k,\delta} - [\alpha_h(V^{k,\delta})+\beta_h(V^{k,\delta})]R^{k,\delta} = -cg_{Na}^{k,\delta}\big(m^{k,\delta}\big)^b\big(h^{k,\delta}\big)^{c-1}(V^{k,\delta}-V_{Na})U^{k,\delta}, \\
U^{k,\delta}(T)=0, \quad P^{k,\delta}(T)=0, \quad Q^{k,\delta}(T)=0, \quad R^{k,\delta}(T)=0,
\end{cases}
\tag{22}
$$

where the derivatives of $\alpha_m, \alpha_n, \alpha_h, \beta_m, \beta_n$ and β_h with respect to V are given by

$$
\begin{aligned}
\alpha_m'(V) &= 0.01\frac{10+(15-V)\exp((25-V)/10)}{(\exp((25-V)/10)-1)^2}, & \beta_m'(V) &= -\frac{2}{9}\exp(-V/18), \\
\alpha_n'(V) &= 0.001\frac{10-V\exp((10-V)/10)}{(\exp((10-V)/10)-1)^2}, & \beta_n'(V) &= -\frac{0.125}{80}\exp(-V/80), \\
\alpha_h'(V) &= -\frac{0.07}{20}\exp(-V/20), & \beta_h'(V) &= 0.1\frac{V\exp((30-V)/10)}{(\exp((30-V)/10)+1)^2}.
\end{aligned}
$$

Proof: See Appendix A.

Given an initial approximation $\boldsymbol{g}^{1,\delta}$ and V^δ, we obtain a regularizing approximation $\boldsymbol{g}^{k_*,\delta}$ for $\boldsymbol{g}$, from minimal error iteration (see Eqs. (16) and (17)).

We next describe the computational scheme.

Algorithm 1: Minimal error iteration to obtain conductances. The norm $\|\cdot\|_{\mathbb{R}^J} \approx \|\cdot\|_{L^2[0,T]}$ is defined in Eq. (23). The ODEs (21) and (22) are solved with a finite difference method, and we obtain numerical solutions $\boldsymbol{V}^{k,\delta} \approx V^{k,\delta}$, $\boldsymbol{m}^{k,\delta} \approx m^{k,\delta}$, $\boldsymbol{n}^{k,\delta} \approx n^{k,\delta}$, $\boldsymbol{h}^{k,\delta} \approx h^{k,\delta}$ and $\boldsymbol{U}^{k,\delta} \approx U^{k,\delta}$. The numerical solution from ODE (11) is $\boldsymbol{V} \approx V$, the parameter $\boldsymbol{V}^{\delta}$ is an approximation of $\boldsymbol{V}$, satisfying Eq. (28). We use the trapezoidal rule to estimate the integral.

Data:
Parameters: a, b, c, V_{Na} ,V_{K}, V_l, C_M, I_{ext}, T, V^{δ}, δ and τ
ODE initial condition: V_0
Initial approximation: $\boldsymbol{g}^{1,\delta}$
Result: Compute an approximation for $\boldsymbol{g}$ using minimal error iteration scheme
k=1;
Compute m_0, n_0, h_0 from Eq. (10);
Compute $m^{1,\delta}$, $n^{1,\delta}$, $h^{1,\delta}$ and $V^{1,\delta}$ from Eq. (21), replacing $\boldsymbol{g}^{k,\delta}$ by $\boldsymbol{g}^{1,\delta}$;
while $\tau\delta \leq \|V^{\delta} - V^{k,\delta}\|_{L^2(0,T)}$ **do**
    Compute $U^{k,\delta}$ from Eq. (22);
    Compute $\boldsymbol{g}^{k+1,\delta}$ using Eq. (17);
    Compute $m^{k+1,\delta}$, $n^{k+1,\delta}$, $h^{k+1,\delta}$ and $V^{k+1,\delta}$ from Eq. (21), replacing $\boldsymbol{g}^{k,\delta}$ by $\boldsymbol{g}^{k+1,\delta}$;
    $k \leftarrow k+1$;
end

Remark 2. *Each* while-loop *of the Algorithm 1 involves solving two nonlinear systems of ODEs. Of course, there is no analytical solution for those equations, and the use of numerical methods is necessary. We use explicit Euler method with a fixed time step Δt to find approximate values of the systems of ODEs. Accordingly, the norms involved in the estimation are discrete approximations of the $L^2(0,T)$ norm. We discretize the time variable $t_j = (j-1)\Delta t$ for $j = 1, 2, \ldots, J$, with time steps $\Delta t = T/(J-1)$. The points $V_j = V(t_j)$, for all $j = 1, 2, \ldots, J$. We denote $\boldsymbol{V} = (V_1, V_2, \ldots, V_J)$ and $\boldsymbol{x} = (x_1, x_2, x_3)$, and consider*

$$\|V\|^2_{L^2[0,T]} \approx \|\boldsymbol{V}\|^2_{l^2} := \Delta t \|\boldsymbol{V}\|^2_{\mathbb{R}^J} = \Delta t \sum_{j=1}^{J} |V(t_j)|^2. \tag{23}$$

2.2. **Inverse Problem to obtain exponents in the H–H model.** Assume again that (11) holds and that g_{K}, g_{Na} and g_l are known. The goal of this subsection is to estimate the exponents a, b and c in the system of ODEs (11). Denoting the unknown parameters by $\boldsymbol{x} = \boldsymbol{a} = (a, b, c)$ it follows from iteration (14) that

$$\boldsymbol{a}^{k+1,\delta} = \boldsymbol{a}^{k,\delta} + w^{k,\delta} F'(\boldsymbol{a}^{k,\delta})^*(V^{\delta} - V^{k,\delta}), \tag{24}$$

where $\boldsymbol{a}^{k,\delta} = (a^{k,\delta}, b^{k,\delta}, c^{k,\delta})$.

In Theorem 2.2, we calculate the action of the unknown operator $F'(\boldsymbol{a}^{k,\delta})^*$, and obtain the Algorithm (25).

Theorem 2.2. *Assume that g_K, g_{Na}, g_l, V_{Na} ,V_K, V_l, C_M, I_{ext}, V_0, m_0, n_0, h_0 and T are known data. Assume also that V^{δ}, $V^{k,\delta}$ and $\boldsymbol{g}^{k,\delta} = (g_K^{k,\delta}, g_{Na}^{k,\delta}, g_l^{k,\delta})$ are known, and that $V^{\delta} = F(\boldsymbol{g}^{\delta})$ and*

$V^{k,\delta} = F(\boldsymbol{g}^{k,\delta})$. *Then*

$$F'(\boldsymbol{a}^{k,\delta})^*(V^\delta - V^{k,\delta}) = \left(X_a^{k,\delta}, X_b^{k,\delta}, X_c^{k,\delta}\right), \tag{25}$$

where

$$\begin{aligned} X_a^{k,\delta} &= \int_0^T g_K(V^{k,\delta} - V_K)\big(n^{k,\delta}\big)^{a^{k,\delta}} U^{k,\delta} \ln(n^{k,\delta})\,dt, \\ X_b^{k,\delta} &= \int_0^T g_{Na}(V^{k,\delta} - V_{Na})\big(m^{k,\delta}\big)^{b^{k,\delta}} \big(h^{k,\delta}\big)^{c^{k,\delta}} U^{k,\delta} \ln(m^{k,\delta})\,dt, \\ X_c^{k,\delta} &= \int_0^T g_{Na}(V^{k,\delta} - V_{Na})\big(m^{k,\delta}\big)^{b^{k,\delta}} \big(h^{k,\delta}\big)^{c^{k,\delta}} U^{k,\delta} \ln(h^{k,\delta})\,dt. \end{aligned}$$

The functions $m^{k,\delta}$, $n^{k,\delta}$, $h^{k,\delta}$ *and* $V^{k,\delta}$ *solve*

$$\begin{cases} I_{ext} = C_M \dot{V}^{k,\delta} + g_K\big(n^{k,\delta}\big)^{a^{k,\delta}}(V^{k,\delta} - V_K) + g_{Na}\big(m^{k,\delta}\big)^{b^{k,\delta}}\big(h^{k,\delta}\big)^{c^{k,\delta}}(V^{k,\delta} - V_{Na}) \\ \qquad\qquad + g_l(V^{k,\delta} - V_l), \\ \dot{\mathcal{X}}^{k,\delta} = (1 - \mathcal{X}^{k,\delta})\alpha_{\mathcal{X}}(V^{k,\delta}) - \mathcal{X}^{k,\delta}\beta_{\mathcal{X}}(V^{k,\delta}); \quad \mathcal{X} = m, n, h, \\ V^{k,\delta}(0) = V_0, \quad m^{k,\delta}(V_0, 0) = m_0, \quad n^{k,\delta}(V_0, 0) = n_0, \quad h^{k,\delta}(V_0, 0) = h_0, \end{cases} \tag{26}$$

where $a^{k,\delta}$, $b^{k,\delta}$ *and* $c^{k,\delta}$ *are given. Also,* $U^{k,\delta}$ *solves*

$$\begin{cases} C_M \dot{U}^{k,\delta} - \left(g_K\big(n^{k,\delta}\big)^{a^{k,\delta}} + g_{Na}\big(m^{k,\delta}\big)^{b^{k,\delta}}\big(h^{k,\delta}\big)^{c^{k,\delta}} + g_l\right) U^{k,\delta} \\ \qquad -[(1 - m^{k,\delta})\alpha'_m(V^{k,\delta}) - m^{k,\delta}\beta'_m(V^{k,\delta})]P^{k,\delta} \\ \qquad -[(1 - n^{k,\delta})\alpha'_n(V^{k,\delta}) - n^{k,\delta}\beta'_n(V^{k,\delta})]Q^{k,\delta} \\ \qquad -[(1 - h^{k,\delta})\alpha'_h(V^{k,\delta}) - h^{k,\delta}\beta'_h(V^{k,\delta})]R^{k,\delta} = V^\delta - V^{k,\delta}, \\ \dot{P}^{k,\delta} - [\alpha_m(V^{k,\delta}) + \beta_m(V^{k,\delta})]P^{k,\delta} = \\ \qquad -b^{k,\delta} g_{Na}\big(m^{k,\delta}\big)^{b^{k,\delta}-1}\big(h^{k,\delta}\big)^{c^{k,\delta}}(V^{k,\delta} - V_{Na})U^{k,\delta}, \\ \dot{Q}^{k,\delta} - [\alpha_n(V^{k,\delta}) + \beta_n(V^{k,\delta})]Q^{k,\delta} = \\ \qquad -a^{k,\delta} g_K\big(n^{k,\delta}\big)^{a^{k,\delta}-1}(V^{k,\delta} - V_K)U^{k,\delta}, \\ \dot{R}^{k,\delta} - [\alpha_h(V^{k,\delta}) + \beta_h(V^{k,\delta})]R^{k,\delta} = \\ \qquad -c^{k,\delta} g_{Na}\big(m^{k,\delta}\big)^{b^{k,\delta}}\big(h^{k,\delta}\big)^{c^{k,\delta}-1}(V^{k,\delta} - V_{Na})U^{k,\delta}, \\ U^{k,\delta}(T) = 0; \quad P^{k,\delta}(T) = 0; \quad R^{k,\delta}(T) = 0; \quad Q^{k,\delta}(T) = 0, \end{cases} \tag{27}$$

given $m^{k,\delta}$, $n^{k,\delta}$, $h^{k,\delta}$ *and* $V^{k,\delta}$. *The constants* G_{Na}, G_K, V_{Na} ,V_K, E_L, C_M, I_{ext}, m_0, n_0 *and* h_0 *are given data.*

Proof: See Appendix (B).

We next describe the computational scheme. Given an initial approximation $\boldsymbol{a}^{1,\delta}$ and V^{δ}, we obtain a regularizing approximation $\boldsymbol{a}^{k_*,\delta}$ for $\boldsymbol{a}$, from minimal error iteration (see Eqs. (24) and (25)).

Algorithm 2: Minimal error iteration to obtain exponents. The norm $\|\cdot\|_{\mathbb{R}^J} \approx \|\cdot\|_{L^2[0,T]}$ is defined in Eq. (23). The ODEs (26) and (27) are solved with a finite difference method, and we obtain numerical solutions $\boldsymbol{V}^{k,\delta} \approx V^{k,\delta}$, $\boldsymbol{m}^{k,\delta} \approx m^{k,\delta}$, $\boldsymbol{n}^{k,\delta} \approx n^{k,\delta}$, $\boldsymbol{h}^{k,\delta} \approx h^{k,\delta}$ and $\boldsymbol{U}^{k,\delta} \approx U^{k,\delta}$. The numerical solution from ODE (11) is $\boldsymbol{V} \approx V$, the parameter $\boldsymbol{V}^{\delta}$ is an approximation of $\boldsymbol{V}$, satisfying Eq. (28).

Data:
Parameters: g_{K}, g_{Na}, g_l, V_{K} ,V_{Na}, V_l, C_M, I_{ext}, T, V^{δ}, δ and τ
ODE initial condition: V_0
Initial approximation: $\boldsymbol{a}^{1,\delta}$
Result: Compute an approximation for $\boldsymbol{a}$ using minimal error iteration scheme
k=1;
Compute m_0, n_0, h_0 from Eq. (10);
Compute $m^{1,\delta}$, $n^{1,\delta}$, $h^{1,\delta}$ and $V^{1,\delta}$ from Eq. (21), replacing $\boldsymbol{a}^{k,\delta}$ by $\boldsymbol{a}^{1,\delta}$;
while $\tau\delta \leq \|V^{\delta} - V^{k,\delta}\|_{L^2(0,T)}$ **do**
  Compute $U^{k,\delta}$ from Eq. (27);
  Compute $\boldsymbol{a}^{k+1,\delta}$ using Eq. (25);
  Compute $m^{k+1,\delta}$, $n^{k+1,\delta}$, $h^{k+1,\delta}$ and $V^{k+1,\delta}$ from Eq. (26), replacing $\boldsymbol{a}^{k,\delta}$ by $\boldsymbol{a}^{k+1,\delta}$;
  $k \leftarrow k+1$;
end

3. NUMERICAL SIMULATION

To design our numerical experiments, we first choose $\boldsymbol{x}$ ($\boldsymbol{x} = \boldsymbol{g}$ or $\boldsymbol{x} = \boldsymbol{a}$) and approximate $\boldsymbol{V}$ from (11) using the explicit Euler method, with a fixed time step Δt. Of course, in practice, the values of $\boldsymbol{V}$ are given by some experimental measurements, and thus subject to experimental/measurement errors. Thus, for a fixed and positive ε, we perform M experiments, where in the i-th experiment we obtain $\boldsymbol{V}^{\delta_i} = (V_1^{\delta_i}, V_2^{\delta_i}, \ldots, V_J^{\delta_i})$ by adding multiplicative and additive noise as

$$V_j^{\delta_i} = V_j + (V_j + 1)\,\mathrm{rand}_j^{\varepsilon}, \quad \text{for all } j = 1, 2, \ldots, J, \tag{28}$$

where $\mathrm{rand}_j^{\varepsilon}$ is a uniformly distributed random variable taking values in the range $[-\varepsilon, \varepsilon]$.

From Eqs. (13) and (28), let, for $i = 1, \ldots, M$,

$$\delta_i = \|\boldsymbol{V} - \boldsymbol{V}^{\delta_i}\|_{l^2} = \Delta t \sqrt{\sum_{j=1}^{J} (V_j + 1)^2 (\mathrm{rand}_j^{\varepsilon})^2} \leq \varepsilon \|\boldsymbol{V} + 1\|_{l^2}, \tag{29}$$

where $\boldsymbol{V} + 1$ denotes the vector with components $V_j + 1$. Note that we replace δ for δ_i in Algorithms 1 and 2, and we define ε to make the perturbation of the voltage $\boldsymbol{V}$ (see Eq. 28).

For each experiment, from Eqs. (15) and (23), iteration (16) (or iteration (24)) stops after k_* steps, i.e., as soon as

$$\|\boldsymbol{V}^{\delta_i} - \boldsymbol{V}^{k_*,\delta_i}\|_{l^2} \leq \tau \delta_i, \tag{30}$$

where $\tau > 1$ is defined by the user. Note that the stopping criterion depends on δ_i, and that k_* depends on i as well. For the sake of clarity, we do not include that in the notation.

In this section we investigate four different cases. In all instances, we employ a known $\boldsymbol{x}$ to compute $\boldsymbol{V}$. Now, for i-th experimental, we define the voltage $\boldsymbol{V}^{\delta_i}$ using Eq. (28), and obtained the noise level δ_i from Eq. (29). In this paper, we consider $M = 400$ experiments for each fixed ε. Next, we assume $\boldsymbol{V}$ and $\boldsymbol{x}$ unknowns. For each i-th experimental and given the initial guess $\boldsymbol{x}^{1,\delta_i}$, the data $\boldsymbol{V}^{\delta_i}$, and δ_i, we use Algorithm 1 (for $\boldsymbol{x} = \boldsymbol{g}$) or Algorithm 2 (for $\boldsymbol{x} = \boldsymbol{a}$) to obtain $\boldsymbol{x}^{k_*,\delta_i}$, an approximation for $\boldsymbol{x}$. In the process, we also compute $\boldsymbol{V}^{k_*,\delta_i}$, an approximation for $\boldsymbol{V}^{\delta_i}$.

We define the means and standard deviations

$$\begin{aligned} \mu_{x_\ell^\varepsilon} &= \frac{1}{M}\sum_{i=1}^{M} x_\ell^{k_*,\delta_i}, \qquad \sigma_{x_\ell^\varepsilon} = \sqrt{\frac{1}{M}\sum_{i=1}^{M}\left(x_\ell^{k_*,\delta_i} - \mu_{x_\ell^\varepsilon}\right)^2}, \qquad \ell = 1,2,3; \\ \mu_{V_j^{k_*,\varepsilon}} &= \frac{1}{M}\sum_{i=1}^{M} V_j^{k_*,\delta_i}, \qquad \sigma_{V_j^{k_*,\varepsilon}} = \sqrt{\frac{1}{M}\sum_{i=1}^{M}\left(V_j^{k_*,\delta_i} - \mu_{V_j^{k_*,\varepsilon}}\right)^2}, \qquad j = 1,2,\dots,J. \end{aligned} \tag{31}$$

We denote $\mu_{\boldsymbol{x}^\varepsilon} = (\mu_{x_1^\varepsilon}, \mu_{x_2^\varepsilon}, \mu_{x_3^\varepsilon})$, $\sigma_{\boldsymbol{x}^\varepsilon} = (\sigma_{x_1^\varepsilon}, \sigma_{x_2^\varepsilon}, \sigma_{x_3^\varepsilon})$, $\mu_{\boldsymbol{V}^{k_*,\varepsilon}} = (\mu_{V_1^{k_*,\varepsilon}}, \mu_{V_2^{k_*,\varepsilon}}, \dots, \mu_{V_J^{k_*,\varepsilon}})$, and $\sigma_{\boldsymbol{V}^{k_*,\varepsilon}} = (\sigma_{V_1^{k_*,\varepsilon}}, \sigma_{V_2^{k_*,\varepsilon}}, \dots, \sigma_{V_J^{k_*,\varepsilon}})$.

$$\begin{aligned} &\bar{\mu}_\varepsilon = \frac{1}{M}\sum_{i=1}^{M}\|\boldsymbol{V}^{\delta_i} - \boldsymbol{V}\|_{l^2}, \quad \tilde{\mu}_\varepsilon = \frac{1}{M}\sum_{i=1}^{M}\|\boldsymbol{V}^{\delta_i} - \boldsymbol{V}^{k_*,\delta_i}\|_{l^2}, \quad \hat{\mu}_\varepsilon = \frac{1}{M}\sum_{i=1}^{M}\|\boldsymbol{V} - \boldsymbol{V}^{k_*,\delta_i}\|_{l^2}, \\ &\mu_\varepsilon = \|\boldsymbol{V} - \mu_{\boldsymbol{V}^{k_*,\varepsilon}}\|_{l^2} \quad \text{and} \quad \text{Error}_{\boldsymbol{x}} = \frac{\|\boldsymbol{x} - \mu_{\boldsymbol{x}^\varepsilon}\|_{l^2}}{\|\boldsymbol{x}\|_{l^2}} \times 100\%. \end{aligned} \tag{32}$$

In Examples 3.1 and 3.2, we estimate the conductances g_{K}, g_{Na} and g_l, and in Examples 3.3 and 3.4, we estimate the exponents a, b and c. In Examples 3.1 and 3.3, all parameters were taken from (Hodgkin and Huxley, 1952). In Examples 3.2 and 3.4, we also consider the parameters from (Hodgkin and Huxley, 1952), except g_{K}, g_{Na} and g_l for Example 3.2 and a, b and c for Example 3.4.

In the following, we set the parameter values for the system of ODEs (11), according to (Hodgkin and Huxley, 1952). For all examples computed: $C_M = 1$ $[\mu F/cm^2]$, $V_{\text{K}} = -12$ $[mV]$, $V_{\text{Na}} = 115$ $[mV]$, $V_l = 10.61$ $[mV]$, $\Delta t = 0.01$ $[ms]$ and $T = 10$ $[ms]$. For Examples 3.1 and 3.2, $\boldsymbol{a} = (4,3,1)$. For Examples 3.3 and 3.4, $\boldsymbol{g} = (36, 120, 0.3)$ $[mS/cm^2]$.

For all our numerical tests, we consider $V_0 = -10$ $[mV]$ and $I_{\text{ext}} = 30$ $[\mu A/cm^2]$. Initial conditions m_0, n_0 and h_0 are obtained from Eq. (10). In our numerical scheme we set the initial guess $\boldsymbol{x}^{1,\delta} = (0,0,0)$ and $\tau = 1.02$, where $\boldsymbol{x}^{1,\delta} = \boldsymbol{g}^{1,\delta}$ or $\boldsymbol{x}^{1,\delta} = \boldsymbol{a}^{1,\delta}$.

Our simulation were computed with Matlab R2019a on a Dell PC, running on a Intel(R) Core(TM) i7-4790 CPU @ 3.60GHz with 16 GB of RAM. The code was made available at `https://github.com/MandujanoValle/Conductances-HH`, to estimate the conductances g_{K}, g_{Na} and g_l, and URL:`https://github.com/MandujanoValle/Exponents-HH`, to estimate the exponents a, b and c.

Example 3.1. *In this numerical test we follow (Hodgkin and Huxley, 1952) and set the maximum conductances as* $\boldsymbol{g} = (g_{Na}, g_K, g_l) = (120, 36, 0.3)$ $[mS/cm^2]$. *We next consider* $\boldsymbol{g}$ *unknown and approximate it using* $\boldsymbol{V}^\delta$ *generated for various values of* ε.

The minimal error method yielded good estimates, in this case, as displayed in Table 2. For example, for 5% *of noise in the membrane potential measurements we obtain* $g_{Na} = 119.34$ $[mS/cm^2]$, $g_K = 35.98$ $[mS/cm^2]$ *and* $g_l = 0.28$ $[mS/cm^2]$. *At each line of the table, the noise is reduced by a factor two.*

In Figure 1, we show the mean $\mu_{\boldsymbol{V}^{k_*,\varepsilon}}$ *and standard deviation* $\sigma_{\boldsymbol{V}^{k_*,\varepsilon}}$ *of the membrane potential approximations for* $\varepsilon = 10\%$ *of noise and with* $M = 400$. *We also present the difference between* $\boldsymbol{V}$ *and* $\mu_{\boldsymbol{V}^{k_*,\varepsilon}}$. *In Figure 2, we display the means, standard deviations and histograms of the maximum conductances approximations.*

Example 3.2. *The pyramidal neuron in the rat hippocampus has maximum conductances* $\boldsymbol{g} = (100, 80, 0.1)$ $[mS/cm^2]$ *(Börgers, 2017), and we use that to generate the noisy data* $\boldsymbol{V}^\delta$ *for various values of* ϵ. *Now, we consider* $\boldsymbol{g}$ *as unknown. Table 3 shows results of method when we try to recover the exact* $\boldsymbol{g}$*, for the various noise levels.*

In Figures 3 and 4, we plot numerical results for $\varepsilon = 10\%$ *of noise with* $M = 400$ *experiments (see Table 3, line 4). Comparing Figure 1-A (Example 3.1) and Figure 3-A from the present example, we see that the membrane potential for each example does not change much, but the conductances undergo a considerable variation.*

Example 3.3. *We now consider the problem of figuring out what are the correct exponents for the H–H model. Following (Hodgkin and Huxley, 1952), we set* $\boldsymbol{a} = (4, 3, 1)$ *and generate noisy membrane potential. These parameters were determined by (Hodgkin and Huxley, 1952) assuming the sodium and potassium conductance curves. Next, we consider* $\boldsymbol{a}$ *unknown.*

Given the measurement of the membrane potential $\boldsymbol{V}^{\delta_i}$*, we estimate the unknown parameter* $\boldsymbol{g}$ *using our proposed approach. In Table 4, we show good estimates for various noise levels, for example, for* $\varepsilon = 5\%$ *of noise we estimate* $\boldsymbol{a} = (3.94, 2, 99, 0.99)$. *As we can see in this table, the relative error of the estimate* $(Error_{\boldsymbol{a}})$ *is approximately one quarter of the noise level, i. e., for* $\varepsilon = 5\%$ *we have* $Error_{\boldsymbol{a}} = 1.2\%$.

In figures 5 and 6, we plot results for $\varepsilon = 10\%$ *of noise with* $M = 400$ *experiments (Table 4, line 4).*

Example 3.4. *One of the most fundamental models in computational neuroscience is the* I_A*-model (Izhikevich, 2007). This formulation considers* $\boldsymbol{a} = (a, b, c) = (0, 1, 1)$*, and we use these value to generate the membrane potential with added noise. Now, we consider* $\boldsymbol{a}$ *unknown.*

In Table 5 shows the algorithm results when approximating $\boldsymbol{a}$*, given the noise levels* ε. *In Figures 7 and 8, we plot numerical results for* $\varepsilon = 10\%$ *of noise with* $M = 400$ *experiments (see Table 5, line 4).*

In all above examples, we estimate the unknown parameters based only on measurements of the membrane potential and without using the conductances G_{K} and G_{Na}.

In the following, we describe the results of Tables 2-5. For all tables, the first column contains the maximum noise level ε at each point of the voltage, and for each line of the tables, the noise is reduced by a factor two. In the second column, for each fixed ε, we present the average of the noise levels $\bar{\mu}_\varepsilon$. This measure is the average of the absolute errors between the measurements $\boldsymbol{V}^{\delta_i}$ and exact voltage $\boldsymbol{V}$. The third column describes the average of the absolute errors between the

ε	$\bar{\mu}_\varepsilon$	$\tilde{\mu}_\varepsilon$	$\hat{\mu}_\varepsilon$	μ_ε	Error$_{\boldsymbol{g}}$	$\mu_{\boldsymbol{g}} = (\mu_{g_{\text{Na}}}, \mu_{g_{\text{K}}}, \mu_{g_l})$
40%	29.64	30.19	6.53	5.21	6.6 %	(111.79, 35.65, 0.15)
20%	14.81	15.08	3.28	2.52	2.7 %	(116.65, 36.11, 0.24)
10%	7.41	7.54	1.65	1.21	1.1 %	(118.59, 36.01, 0.26)
5%	3.70	3.77	0.80	0.61	0.5 %	(119.34, 35.98, 0.28)

TABLE 2. Numerical results for Example 3.1 with $M = 400$ experiments for each noise level ε. The first column describes the noise level, as in Eq. (28). The second, third and four columns are the arithmetic mean, see Eq. (32). The second column represents the average of the measurement errors. The third column shows the average of the errors between the measurements $\boldsymbol{V}^{\delta_i}$ and the approximations $\boldsymbol{V}^{k_*,\delta_i}$, these last values are obtained by the proposed method. The fourth column is the average of the errors between the exact value $\boldsymbol{V}$ and the approximations $\boldsymbol{V}^{k_*,\delta_i}$. The fifth column shows the error between the exact value $\boldsymbol{V}$ and the average approximations $\mu_{\boldsymbol{V}^{k_*,\varepsilon}}$. The sixth column is the estimation error for $\boldsymbol{x} = \boldsymbol{g}$, see Eq. (32). Finally, the last column shows the approximations for $g_{\text{Na}} = 120$, $g_{\text{K}} = 36$ and $g_l = 0.3$.

ε	$\bar{\mu}_\varepsilon$	$\tilde{\mu}_\varepsilon$	$\hat{\mu}_\varepsilon$	μ_ε	Error$_{\boldsymbol{g}}$	$\mu_{\boldsymbol{g}} = (\mu_{g_{\text{Na}}}, \mu_{g_{\text{K}}}, \mu_{g_l})$
40%	24.64	25.10	5.78	4.71	7.3 %	(92.67, 74.26, 0.004)
20%	12.30	12.53	2.70	2.13	3.2 %	(97.14, 77.05, 0.053)
10%	6.17	6.28	1.40	1.12	1.8 %	(98.41, 78.30, 0.084)
5%	3.09	3.15	0.72	0.57	1.3 %	(98.84, 78.80, 0.091)

TABLE 3. Numerical results for Example 3.2 with $M = 400$ experiments for each noise level ε. In the last column, we estimate $g_{\text{Na}} = 100$, $g_{\text{Na}} = 80$ and $g_l = 0.1$. See Table 2 for a description of the columns.

measurements $\boldsymbol{V}^{\delta_i}$ and the approximation $\boldsymbol{V}^{k_*,\delta_i}$, and we denote this value by $\tilde{\mu}_\varepsilon$. In all tables, we have $\bar{\mu}_\varepsilon \approx \tilde{\mu}_\varepsilon$, since $\tau = 1.02 \approx 1$; see Eq. (30). The fourth column represents the average of the absolute errors between the exact value $\boldsymbol{V}$ and the approximations $\boldsymbol{V}^{k_*,\delta_i}$, and this value is represented by $\hat{\mu}_\varepsilon$. In all tables, we obtain $\bar{\mu}_\varepsilon \approx 4.5\hat{\mu}_\varepsilon$, because $\boldsymbol{V}^{\delta_i}$ is noisy, and $\boldsymbol{V}$ and $\boldsymbol{V}^{k_*,\delta_i}$ are smooth. The fifth column displays the absolute error between the exact value $\boldsymbol{V}$ and the average of the approximations $\mu_{\boldsymbol{V}^{k_*,\varepsilon}}$, denoted by μ_ε. Note that $\bar{\mu}_\varepsilon \approx 5.3\mu_\varepsilon$, because $\boldsymbol{V}^{\delta_i}$ is noisy, and $\boldsymbol{V}$ and $\mu_{\boldsymbol{V}^{k_*,\varepsilon}}$ are smooth. The sixth column shows the estimation error for $\boldsymbol{x}$, denoted by Error$_{\boldsymbol{x}}$. In all tables, we obtain $\varepsilon/10 \leq \text{Error}_{\boldsymbol{x}} \leq \varepsilon/4$. Finally, the last column presents the mean of $M = 400$ approximations for $\boldsymbol{x}$, represented by $\mu_{\boldsymbol{x}}$.

The histograms, in Figures 2, 4 and 6, approximate the Gaussian distribution when we increase the number of experiments M.

4. CONCLUSIONS

In this paper, we solve two inverse problems related to the H–H model. In the first problem estimate maximum conductances, while in the second one we determine the exponents of the activation and inactivation variables. To calculate the unknown data, we propose the minimal error iteration. The adjoints of some Gateaux derivatives are unknown for each problem, and

ε	$\bar{\mu}_\varepsilon$	$\tilde{\mu}_\varepsilon$	$\hat{\mu}_\varepsilon$	μ_ε	Error$_{\boldsymbol{a}}$	$\mu_{\boldsymbol{a}} = (\mu_a, \mu_b, \mu_c)$
40%	29.64	30.23	6.64	6.09	10.0 %	(3.497, 2.928, 0.959)
20%	14.80	15.10	3.27	2.98	4.8 %	(3.760, 2.974, 0.980)
10%	7.42	7.57	1.64	1.49	2.4 %	(3.880, 2.985, 0.991)
5%	3.70	3.78	0.83	0.75	1.2 %	(3.940, 2.994, 0.995)

TABLE 4. Numerical results for Example 3.3 with $M = 400$ experiments for each noise level ε. In the last column, we estimate $a = 4$, $b = 3$ and $c = 1$. See Table 2 for a description of the columns.

ε	$\bar{\mu}_\varepsilon$	$\tilde{\mu}_\varepsilon$	$\hat{\mu}_\varepsilon$	μ_ε	Error$_{\boldsymbol{a}}$	$\mu_{\boldsymbol{a}} = (\mu_a, \mu_b, \mu_c)$
40%	17.00	17.33	3.79	3.54	7.3 %	(−0.089, 0.950, 0.985)
20%	8.50	8.67	1.94	1.82	3.9 %	(−0.048 ,0.979, 0.991)
10%	4.24	4.33	0.98	0.92	2.0 %	(−0.025, 0.986, 0.996)
5%	2.12	2.16	0.49	0.46	1.0 %	(−0.012, 0.993, 0.998)

TABLE 5. Numerical results for Example 3.4 with $M = 400$ experiments for each noise level ε. In the last column, we estimate $a = 0$, $b = 1$ and $c = 1$. See Table 2 for a description of the columns.

in Appendices A and B, we show how to compute them. This approach solves two systems of nonlinear ordinary differential equations in each iteration. We solve these differential equations with the explicit Euler method, obtaining faster convergences.

The classic Landweber and modified Landweber iterations have $w_k = 1$, for all iterative steps k. In minimal error method, the parameter w_k changes with k. The choice of a different w_k in each iterative step makes the method faster and more stable compared to classic Landweber and modified Landweber iterations. In our numerical tests, the classic Landweber and modified Landweber methods diverged for any noise level, while the minimum error method converged to the exact solution when the noise level goes to zero; cf. Tables 2, 3, 4 and 5.

On the other hand, these gradient-type methods are iterative methods that try to estimate the solution of the inverse problem from an initial guess $\boldsymbol{x}^{1,\delta}$, if this initial condition is far from the exact solution, the algorithm may diverge.

In a series of numerical tests, we show that we can compute approximations for the maximum conductances and activation/inactivation variables under different scenarios. Our methods provide a way to find out parameters that would have to be discovered by trial and error process.

APPENDIX A. PROOF OF THEOREM 2.1

Consider the operator F defined in (12). Then $F(\boldsymbol{g}^{k,\delta}) = V^{k,\delta}$, where $V^{k,\delta}$, $m^{k,\delta}$, $n^{k,\delta}$ and $h^{k,\delta}$ solve the ODE system (21). For $\boldsymbol{\theta} = (\theta_{\text{Na}}, \theta_{\text{K}}, \theta_l) \in \mathbb{R}^3$ and $\lambda \in \mathbb{R}$, then $F(\boldsymbol{g}^{k,\delta} + \lambda\boldsymbol{\theta}) = V_\lambda^{k,\delta}$, where $V_\lambda^{k,\delta}$, $m_\lambda^{k,\delta}$, $n_\lambda^{k,\delta}$ and $h_\lambda^{k,\delta}$ solve

$$
\left\{
\begin{aligned}
& I_{\text{ext}} = C_M \dot{V}_\lambda^{k,\delta} + \left(g_{\text{K}}^{k,\delta} + \lambda\theta_K\right)\left(n_\lambda^{k,\delta}\right)^a \left(V_\lambda^{k,\delta} - V_{\text{K}}\right) \\
& \quad + \left(g_{\text{Na}}^{k,\delta} + \lambda\theta_{\text{Na}}\right)\left(m_\lambda^{k,\delta}\right)^b \left(h_\lambda^{k,\delta}\right)^c \left(V_\lambda^{k,\delta} - V_{\text{Na}}\right) + \left(g_l^{k,\delta} + \lambda\theta_l\right)\left(V_\lambda^{k,\delta} - V_l\right), \\
& \dot{\mathcal{X}}_\lambda^{k,\delta} = (1 - \mathcal{X}_\lambda^{k,\delta})\alpha_{\mathcal{X}}(V_\lambda^{k,\delta}) - \mathcal{X}_\lambda^{k,\delta}\beta_{\mathcal{X}}(V_\lambda^{k,\delta}); \qquad \mathcal{X} = m, n, h, \\
& V_\lambda^{k,\delta}(0) = V_0; \quad m_\lambda^{k,\delta}(0) = m_0; \quad n_\lambda^{k,\delta}(0) = n_0; \quad n_\lambda^{k,\delta}(0) = n_0.
\end{aligned}
\right. \tag{33}
$$

The Gateaux derivative of F at $\boldsymbol{g}^{k,\delta}$ in the direction $\boldsymbol{\theta}$ is given by

$$
W^{k,\delta} = F'(\boldsymbol{g}^{k,\delta})(\boldsymbol{\theta}) = \lim_{\lambda\to 0} \frac{F(\boldsymbol{g}^{k,\delta} + \lambda\boldsymbol{\theta}) - F(\boldsymbol{g}^{k,\delta})}{\lambda}. \tag{34}
$$

Also, we denote the following limits

$$
M^{k,\delta} = \lim_{\lambda\to 0} \frac{m_\lambda^{k,\delta} - m^{k,\delta}}{\lambda}, \quad N^{k,\delta} = \lim_{\lambda\to 0} \frac{n_\lambda^{k,\delta} - n^{k,\delta}}{\lambda}, \quad H^{k,\delta} = \lim_{\lambda\to 0} \frac{h_\lambda^{k,\delta} - h^{k,\delta}}{\lambda}, \tag{35}
$$

where $M^{k,\delta}$, $N^{k,\delta}$ and $H^{k,\delta}$ are the Gateaux derivatives of $m^{k,\delta}$, $n^{k,\delta}$ and $h^{k,\delta}$, respectively.

Considering the difference between ODEs (33) and (21), dividing by λ and taking the limit $\lambda \to 0$, we have the following ODE

$$
\left\{
\begin{aligned}
& C_M \dot{W}^{k,\delta} + \left(g_{\text{K}}^{k,\delta}\left(n^{k,\delta}\right)^a + g_{\text{Na}}^{k,\delta}\left(m^{k,\delta}\right)^b\left(h^{k,\delta}\right)^c + g_l^{k,\delta}\right) W^{k,\delta} = \\
& \quad -a g_{\text{K}}^{k,\delta}\left(n^{k,\delta}\right)^{a-1} N^{k,\delta}(V^{k,\delta} - V_{\text{K}}) - b g_{\text{Na}}^{k,\delta}\left(m^{k,\delta}\right)^{b-1} M^{k,\delta}\left(h^{k,\delta}\right)^c (V^{k,\delta} - V_{\text{Na}}) \\
& \quad -c g_{\text{Na}}^{k,\delta}\left(m^{k,\delta}\right)^b \left(h^{k,\delta}\right)^{c-1} H^{k,\delta}(V^{k,\delta} - V_{\text{Na}}) \\
& \quad -\theta_K\left(n^{k,\delta}\right)^a (V^{k,\delta} - V_{\text{K}}) - \theta_{\text{Na}}\left(m^{k,\delta}\right)^b\left(h^{k,\delta}\right)^c (V^{k,\delta} - V_{\text{Na}}) - \theta_l (V^{k,\delta} - V_l), \\
& \dot{\mathcal{X}}^{k,\delta} + [\alpha_{\mathcal{Y}}(V^{k,\delta}) + \beta_{\mathcal{Y}}(V^{k,\delta})]\mathcal{X}^{k,\delta} = [(1 - \mathcal{Y}^{k,\delta})\alpha'_{\mathcal{Y}}(V^{k,\delta}) - \mathcal{Y}^{k,\delta}\beta'_{\mathcal{Y}}(V^{k,\delta})] W^{k,\delta}; \\
& \ (\mathcal{X}, \mathcal{Y}) = (M, m), (N, n), (H, h), \\
& W^{k,\delta}(0) = 0; \quad M^{k,\delta}(0) = 0; \quad N^{k,\delta}(0) = 0; \quad H^{k,\delta}(0) = 0.
\end{aligned}
\right. \tag{36}
$$

This last equation is yet another system of coupled nonlinear differential equations, depending on the parameter $\boldsymbol{\theta} = (\theta_{\text{Na}}, \theta_K, \theta_l)$, representing an arbitrary point in $\mathbb{R}^3$.

From minimal error iteration (16) and $\boldsymbol{\theta} \in \mathbb{R}^3$ arbitrary, we have

$$
\begin{aligned}
\langle \boldsymbol{g}^{k+1,\delta} - \boldsymbol{g}^{k,\delta}, \boldsymbol{\theta} \rangle_{\mathbb{R}^3} &= w^{k,\delta} \langle F'(\boldsymbol{g}^{k,\delta})^*(V^\delta - F(\boldsymbol{g}^{k,\delta})), \boldsymbol{\theta} \rangle_{\mathbb{R}^3}, \\
&= w^{k,\delta} \langle F'(\boldsymbol{g}^{k,\delta})^*(V^\delta - V^{k,\delta}), \boldsymbol{\theta} \rangle_{\mathbb{R}^3}.
\end{aligned}
$$

By definition of adjoint operator

$$
\langle \boldsymbol{g}^{k+1,\delta} - \boldsymbol{g}^{k,\delta}, \boldsymbol{\theta} \rangle_{\mathbb{R}^3} = w^{k,\delta} \langle V^\delta - V^{k,\delta}, F'(x_k)(\boldsymbol{\theta}) \rangle_{L^2[0,T]}.
$$

From Eq. (34) and the previous equation, we obtain

$$
\langle \boldsymbol{g}^{k+1,\delta} - \boldsymbol{g}^{k,\delta}, \boldsymbol{\theta} \rangle_{\mathbb{R}^3} = w^{k,\delta} \langle V^\delta - V^{k,\delta}, W^{k,\delta} \rangle_{L^2[0,T]}.
$$

The internal product in $L^2[0,T]$ is given by $\langle V^\delta - V^{k,\delta}, W^{k,\delta}\rangle_{L^2[0,T]} = \int_0^T (V^\delta - V^{k,\delta})W^{k,\delta}\, dt$. Denoting the last equality by Φ, we gather that

$$\Phi = \frac{\langle \boldsymbol{g}^{k+1,\delta} - \boldsymbol{g}^{k,\delta}, \boldsymbol{\theta}\ \rangle_{\mathbb{R}^3}}{w^{k,\delta}} = \langle V^\delta - V^{k,\delta}, W^{k,\delta}\rangle_{L^2[0,T]}. \tag{37}$$

From the previous equation and the first equality from ODE (22), we obtain

$$\begin{aligned}\Phi = \int_0^T \Big(C_M \dot{U}^{k,\delta} W^{k,\delta} - \Big(g_{\mathrm{K}}^{k,\delta}\big(n^{k,\delta}\big)^a + g_{\mathrm{Na}}^{k,\delta}\big(m^{k,\delta}\big)^b\big(h^{k,\delta}\big)^c + g_l^{k,\delta}\Big) U^{k,\delta}W^{k,\delta}\Big)\, dt \\ - \int_0^T \big[(1-m^{k,\delta})\alpha_m'(V^{k,\delta}) - m^{k,\delta}\beta_m'(V^{k,\delta})\big]\, P^{k,\delta}W^{k,\delta}\, dt \\ - \int_0^T \big[(1-n^{k,\delta})\alpha_n'(V^{k,\delta}) - n^{k,\delta}\beta_n'(V^{k,\delta})\big]\, Q^{k,\delta}W^{k,\delta}\, dt \\ - \int_0^T \big[(1-h^{k,\delta})\alpha_h'(V^{k,\delta}) - h^{k,\delta}\beta_h'(V^{k,\delta})\big]\, R^{k,\delta}W^{k,\delta}\, dt.\end{aligned} \tag{38}$$

Integrating the first term from (38) by parts, and from the initial $(W^{k,\delta}(0) = 0)$ and final $(U^{k,\delta}(T) = 0)$ conditions, we obtain

$$\int_0^T C_M \dot{U}^{k,\delta} W^{k,\delta} = -\int_0^T C_M U^{k,\delta} \dot{W}^{k,\delta}. \tag{39}$$

Replacing equation (39) in (38), we have

$$\begin{aligned}\Phi \;=\; & -\int_0^T \Big(C_M \dot{W}^{k,\delta} + \Big(g_{\mathrm{K}}^{k,\delta}\big(n^{k,\delta}\big)^a + g_{\mathrm{Na}}^{k,\delta}\big(m^{k,\delta}\big)^b\big(h^{k,\delta}\big)^c + g_l^{k,\delta}\Big) W^{k,\delta}\Big) U^{k,\delta}\, dt \\ & - \int_0^T \big[(1-m^{k,\delta})\alpha_m'(V^{k,\delta}) - m^{k,\delta}\beta_m'(V^{k,\delta})\big]\, P^{k,\delta}W^{k,\delta}\, dt \\ & - \int_0^T \big[(1-n^{k,\delta})\alpha_n'(V^{k,\delta}) - n^{k,\delta}\beta_n'(V^{k,\delta})\big]\, Q^{k,\delta}W^{k,\delta}\, dt \\ & - \int_0^T \big[(1-h^{k,\delta})\alpha_h'(V^{k,\delta}) - h^{k,\delta}\beta_h'(V^{k,\delta})\big]\, R^{k,\delta}W^{k,\delta}\, dt.\end{aligned}$$

Replacing, the first equality from the ODE (36), in the first integral from the previous equation, we gather

$$
\begin{aligned}
\Phi = &+\int_0^T a g_{\mathrm{K}}^{k,\delta}(n^{k,\delta})^{a-1} N^{k,\delta}(V^{k,\delta}-V_{\mathrm{K}})U^{k,\delta}\,dt \\
&\int_0^T b g_{\mathrm{Na}}^{k,\delta}(m^{k,\delta})^{b-1} M^{k,\delta}\big(h^{k,\delta}\big)^c(V^{k,\delta}-V_{\mathrm{Na}})U^{k,\delta}\,dt \\
&+\int_0^T c g_{\mathrm{Na}}^{k,\delta}\big(m^{k,\delta}\big)^b(h^{k,\delta})^{c-1} H^{k,\delta}(V^{k,\delta}-V_{\mathrm{Na}})U^{k,\delta}\,dt \\
&+\int_0^T \big(m^{k,\delta}\big)^b\big(h^{k,\delta}\big)^c(V^{k,\delta}-V_{\mathrm{Na}})\theta_{\mathrm{Na}}U^{k,\delta}\,dt \\
&+\int_0^T \big(n^{k,\delta}\big)^a(V^{k,\delta}-V_{\mathrm{K}})\theta_{\mathrm{K}}U^{k,\delta}\,dt+\int_0^T (V^{k,\delta}-V_l)\theta_l U^{k,\delta}\,dt \\
&-\int_0^T \big[(1-m^{k,\delta})\alpha_m'(V^{k,\delta})-m^{k,\delta}\beta_m'(V^{k,\delta})\big]\,P^{k,\delta}W^{k,\delta}\,dt \\
&-\int_0^T \big[(1-n^{k,\delta})\alpha_n'(V^{k,\delta})-n^{k,\delta}\beta_n'(V^{k,\delta})\big]\,Q^{k,\delta}W^{k,\delta}\,dt \\
&-\int_0^T \big[(1-h^{k,\delta})\alpha_h'(V^{k,\delta})-h^{k,\delta}\beta_h'(V^{k,\delta})\big]\,R^{k,\delta}W^{k,\delta}\,dt.
\end{aligned}
\tag{40}
$$

Multiplying the second equation from (22) by $M^{k,\delta}$, and integrating in the interval $[0,T]$ it follows that

$$
\int_0^T P_t^{k,\delta}M^{k,\delta}-\big[\alpha_m(V^{k,\delta})+\beta_m(V^{k,\delta})\big]\,P^{k,\delta}M^{k,\delta}\,dt = -\int_0^T b g_{\mathrm{Na}}^{k,\delta}\big(m^{k,\delta}\big)^{b-1}\big(h^{k,\delta}\big)^c(V^{k,\delta}-V_{\mathrm{Na}})U^{k,\delta}M^{k,\delta}\,dt.
$$

Integrating by parts the first term from the previous equation, and using the initial $(M^{k,\delta}(0)=0)$ and final $(P^{k,\delta}(T)=0)$ conditions, we have

$$
\int_0^T \Big(\dot M^{k,\delta}+\big[\alpha_m(V^{k,\delta})+\beta_m(V^{k,\delta})\big]\,M^{k,\delta}\Big)\,P^{k,\delta}\,dt = \int_0^T b g_{\mathrm{Na}}^{k,\delta}\big(m^{k,\delta}\big)^{b-1}\big(h^{k,\delta}\big)^c(V^{k,\delta}-V_{\mathrm{Na}})U^{k,\delta}M^{k,\delta}\,dt.
$$

Then, from the previous equation and the second equation from ODE (36), for $(\mathcal{X},\mathcal{Y})=(M,m)$,

$$
\int_0^T b g_{\mathrm{K}}^{k,\delta}\big(m^{k,\delta}\big)^{b-1}\big(h^{k,\delta}\big)^c(V^{k,\delta}-V_{\mathrm{Na}})U^{k,\delta}M^{k,\delta}\,dt = \int_0^T \big[(1-m^{k,\delta})\alpha_m'(V^{k,\delta})-m^{k,\delta}\beta_m'(V^{k,\delta})\big]\,W^{k,\delta}P^{k,\delta}\,dt.
\tag{41}
$$

Multiplying the third equation from (22) by $N^{k,\delta}$, and integrating in the interval $[0,T]$ we gather that

$$\int_0^T \dot{Q}^{k,\delta}N^{k,\delta} - \left[\alpha_n(V^{k,\delta}) + \beta_n(V^{k,\delta})\right] Q^{k,\delta}N^{k,\delta}\, dt = -\int_0^T a g_{\mathrm{K}}^{k,\delta}\left(n^{k,\delta}\right)^{a-1}(V^{k,\delta} - V_{\mathrm{K}})U^{k,\delta}\, dt.$$

Integrating by parts the first term from previous equation, and using the initial $(N^{k,\delta}(0) = 0)$ and final $(Q^{k,\delta}(T) = 0)$ conditions, we have

$$\int_0^T \left(\dot{N}^{k,\delta} + \left[\alpha_n(V^{k,\delta}) + \beta_n(V^{k,\delta})\right] N^{k,\delta}\right) Q^{k,\delta}\, dt = \int_0^T a g_{\mathrm{K}}^{k,\delta}\left(n^{k,\delta}\right)^{a-1}(V^{k,\delta} - V_{\mathrm{K}})U^{k,\delta}\, dt.$$

Then, from the previous equation and the second equation from ODE (36), for $(\mathcal{X},\mathcal{Y}) = (N^{k,\delta}, n^{k,\delta})$, we have

$$\int_0^T a g_{\mathrm{K}}^{k,\delta}\left(n^{k,\delta}\right)^{a-1}(V^{k,\delta} - V_{\mathrm{K}})U^{k,\delta}\, dt = \int_0^T \left[(1-n^{k,\delta})\alpha_n'(V^{k,\delta}) - n^{k,\delta}\beta_n'(V^{k,\delta})\right] W^{k,\delta}Q^{k,\delta}\, dt. \tag{42}$$

Multiplying the fourth equation of (22) by $H^{k,\delta}$, and integrating in the interval $[0,T]$ we gather that

$$\int_0^T \dot{R}^{k,\delta}H^{k,\delta} - \left[\alpha_h(V^{k,\delta}) + \beta_h(V^{k,\delta})\right] R^{k,\delta}H^{k,\delta}\, dt = -\int_0^T c g_{\mathrm{Na}}^{k,\delta}\left(m^{k,\delta}\right)^{b}\left(h^{k,\delta}\right)^{c-1}(V^{k,\delta} - V_{\mathrm{Na}})U^{k,\delta}\, dt.$$

Integrating by parts the first term from the previous equation, and using the initial $(H^{k,\delta}(0) = 0)$ and final $(R^{k,\delta}(T) = 0)$ conditions, we have

$$\int_0^T \left(\dot{H}^{k,\delta} + \left[\alpha_h(V^{k,\delta}) + \beta_h(V^{k,\delta})\right] H^{k,\delta}\right) R^{k,\delta}\, dt = \int_0^T c g_{\mathrm{Na}}^{k,\delta}\left(m^{k,\delta}\right)^{b}\left(h^{k,\delta}\right)^{c-1}(V^{k,\delta} - V_{\mathrm{Na}})U^{k,\delta}\, dt.$$

Then, from the previous equation and the second equation from ODE (36), for $(\mathcal{X},\mathcal{Y}) = (H,h)$, we have

$$\int_0^T c g_{\mathrm{Na}}^{k,\delta}\left(m^{k,\delta}\right)^{b}\left(h^{k,\delta}\right)^{c-1}(V^{k,\delta} - V_{\mathrm{Na}})U^{k,\delta}\, dt = \int_0^T \left[(1-h^{k,\delta})\alpha_h'(V^{k,\delta}) - h^{k,\delta}\beta_h'(V^{k,\delta})\right] W^{k,\delta}R^{k,\delta}\, dt. \tag{43}$$

Substituting equations (41), (42), and (43) in (40), we have

$$\Phi = \int_0^T \left(m^{k,\delta}\right)^b \left(h^{k,\delta}\right)^c (V^{k,\delta} - V_{\text{Na}})\theta_{\text{Na}} U^{k,\delta}\, dt + \int_0^T \left(n^{k,\delta}\right)^a (V^{k,\delta} - V_{\text{K}})\theta_{\text{K}} U^{k,\delta}\, dt + \int_0^T (V^{k,\delta} - V_l)\theta_l U^{k,\delta}\, dt. \tag{44}$$

Substituting equations (19), (18) and (20) in equation (44) we gather that

$$\Phi = X_{\text{Na}}^{k,\delta}\, \theta_{\text{Na}} + X_K^{k,\delta}\, \theta_{\text{K}} + X_l^{k,\delta}\, \theta_l = \left\langle \left(X_{\text{Na}}^{k,\delta}, X_K^{k,\delta}, X_l^{k,\delta}\right), (\theta_{\text{Na}}, \theta_{\text{K}}, \theta_l) \right\rangle_{\mathbb{R}^3}. \tag{45}$$

From (37) and (45)

$$\frac{\langle \boldsymbol{g}^{k+1,\delta} - \boldsymbol{g}^{k,\delta}, \boldsymbol{\theta} \rangle_{\mathbb{R}^3}}{w^{k,\delta}} = \left\langle \left(X_{\text{Na}}^{k,\delta}, X_K^{k,\delta}, X_l^{k,\delta}\right), \boldsymbol{\theta} \right\rangle_{\mathbb{R}^3}.$$

Since $\boldsymbol{\theta} \in \mathbb{R}^3$ is arbitrary, we obtain (17).

Appendix B. Proof of Theorem 2.2

Let F be as in (12). Then $F(\boldsymbol{a}^{k,\delta}) = V^{k,\delta}$, where $V^{k,\delta}$, $m^{k,\delta}$, $n^{k,\delta}$ and $h^{k,\delta}$ solve the ODE system (26). Let $\boldsymbol{\theta} = (\theta_a, \theta_b, \theta_c) \in \mathbb{R}^3$ and $\lambda \in \mathbb{R}$, then $F(\boldsymbol{a}^{k,\delta} + \lambda\boldsymbol{\theta}) = V_\lambda^{k,\delta}$, where $V_\lambda^{k,\delta}$, $m_\lambda^{k,\delta}$, $n_\lambda^{k,\delta}$ and $h_\lambda^{k,\delta}$ solve

$$\begin{cases} C_M \dot{V}_\lambda^{k,\delta} = I_{\text{ext}} - g_{\text{K}}^{k,\delta}\left(n_\lambda^{k,\delta}\right)^{a^{k,\delta}+\lambda\theta_a}\left(V_\lambda^{k,\delta} - V_{\text{K}}\right) \\ \quad -g_{\text{Na}}\left(m_\lambda^{k,\delta}\right)^{b^{k,\delta}+\lambda\theta_b}\left(h_\lambda^{k,\delta}\right)^{c^{k,\delta}+\lambda\theta_c}\left(V_\lambda^{k,\delta} - V_{\text{Na}}\right) - g_l\left(V_\lambda^{k,\delta} - V_l\right), \\ \dot{\mathcal{X}}_\lambda^{k,\delta} = (1 - \mathcal{X}_\lambda^{k,\delta})\alpha_{\mathcal{X}}(V^{k,\delta}) - \mathcal{X}_\lambda^{k,\delta}\beta_{\mathcal{X}}(V^{k,\delta}), \quad \text{for } \mathcal{X} = m, n, h, \\ V_\lambda^{k,\delta}(0) = V_0, \quad m_\lambda^{k,\delta}(0) = m_0, \quad n_\lambda^{k,\delta}(0) = n_0, \quad n_\lambda^{k,\delta}(0) = n_0. \end{cases} \tag{46}$$

Considering the difference between the ODEs (46) and (26), dividing by λ and taking the limit $\lambda \to 0$, we have the ODE

$$\begin{cases} C_M \dot{W}^{k,\delta} + \left(g_{\text{K}}\left(n^{k,\delta}\right)^{a^{k,\delta}} + g_{\text{Na}}\left(m^{k,\delta}\right)^{b^{k,\delta}}\left(h^{k,\delta}\right)^{c^{k,\delta}} + g_l\right) W^{k,\delta} = \\ \quad -b^{k,\delta} g_{\text{Na}}\left(m^{k,\delta}\right)^{b^{k,\delta}-1} M^{k,\delta}\left(h^{k,\delta}\right)^{c^{k,\delta}}(V^{k,\delta} - V_{\text{Na}}) \\ \quad -\mathsf{b} g_{\text{Na}}\left(m^{k,\delta}\right)^{b^{k,\delta}}\left(h^{k,\delta}\right)^{c^{k,\delta}-1} H^{k,\delta}(V^{k,\delta} - V_{\text{Na}}) \\ \quad -a^{k,\delta} g_{\text{K}}\left(n^{k,\delta}\right)^{a^{k,\delta}-1} N^{k,\delta}(V^{k,\delta} - V_{\text{K}}) \\ \quad -g_{\text{Na}}\left(m^{k,\delta}\right)^{b^{k,\delta}} \ln(m^{k,\delta})\left(h^{k,\delta}\right)^{c^{k,\delta}}(V^{k,\delta} - V_{\text{Na}})\theta_b \\ \quad -g_{\text{Na}}\left(m^{k,\delta}\right)^{b^{k,\delta}}\left(h^{k,\delta}\right)^{c^{k,\delta}} \ln(h^{k,\delta})(V^{k,\delta} - V_{\text{Na}})\theta_c \\ \quad -g_k\left(n^{k,\delta}\right)^b \ln(n^{k,\delta})(V^{k,\delta} - V_{\text{K}})\theta_a, \\ \dot{\mathcal{X}}^{k,\delta} + [\alpha_{\mathcal{Y}}(V^{k,\delta}) + \beta_{\mathcal{Y}}(V^{k,\delta})]\mathcal{X}^{k,\delta} = [(1 - \mathcal{Y}^{k,\delta})\alpha'_{\mathcal{Y}}(V^{k,\delta}) - \mathcal{Y}^{k,\delta}\beta'_{\mathcal{Y}}(V^{k,\delta})]W^{k,\delta}, \\ \quad (\mathcal{X}, \mathcal{Y}) = (M, m), (N, n), (H, h), \\ W^{k,\delta}(0) = 0, \quad M^{k,\delta}(0) = 0, \quad N^{k,\delta}(0) = 0, \quad H^{k,\delta}(0) = 0. \end{cases} \tag{47}$$

where $W^{k,\delta}$ is defined in equation (34) by replacing $\boldsymbol{g}^{k,\delta}$ by $\boldsymbol{a}^{k,\delta}$. Also, $M^{k,\delta}$, $N^{k,\delta}$ and $H^{k,\delta}$ are defined in equation (35).

This last equation is again a system of coupled nonlinear differential equations, parametrized by $\boldsymbol{\theta} = (\theta_a, \theta_b, \theta_c)$, where $\boldsymbol{\theta} \in \mathbb{R}^3$ is arbitrary. Considering (27), and proceeding as in Appendix A, we gather (25).

Appendix C. Supplementary material

Supplementary material associated with this article can be found at `https://raw.githubusercontent.com/MandujanoValle/Teste/master/Supplementary.pdf`

References

Avdonin, S. and Bell, J. (2013). Determining a distributed parameter in a neural cable model via a boundary control method. *Journal of mathematical biology*, 67(1):123–141.

Avdonin, S. and Bell, J. (2015). Determining a distributed conductance parameter for a neuronal cable model defined on a tree graph. *Journal of Inverse Problems and Imaging*, 9:645–659.

Bell, J. and Craciun, G. (2005). A distributed parameter identification problem in neuronal cable theory models. *Mathematical biosciences*, 194(1):1–19.

Benning, M. and Burger, M. (2018). Modern regularization methods for inverse problems. *Acta Numerica*, 27:1–111.

Binder, A., Hanke, M., and Scherzer, O. (1996). On the Landweber iteration for nonlinear ill-posed problems. *Journal of Inverse and Ill-posed Problems*, 4(5):381–390.

Bojak, I., Oostendorp, T. F., Reid, A. T., and Kötter, R. (2010). Connecting mean field models of neural activity to EEG and fMRI data. *Brain topography*, 23(2):139–149.

Börgers, C. (2017). *An introduction to modeling neuronal dynamics*, volume 66. Springer.

Bower, J. M. and Beeman, D. (2012). *The book of GENESIS: exploring realistic neural models with the GEneral NEural SImulation System*. Springer Science & Business Media.

Buhry, L., Grassia, F., Giremus, A., Grivel, E., Renaud, S., and Saïghi, S. (2011). Automated parameter estimation of the Hodgkin-Huxley model using the differential evolution algorithm: application to neuromimetic analog integrated circuits. *Neural computation*, 23(10):2599–2625.

Buhry, L., Pace, M., and Saïghi, S. (2012). Global parameter estimation of an Hodgkin–Huxley formalism using membrane voltage recordings: Application to neuro-mimetic analog integrated circuits. *Neurocomputing*, 81:75–85.

Buzsáki, G., Anastassiou, C. A., and Koch, C. (2012). The origin of extracellular fields and currents-EEG, ECoG, LFP and spikes. *Nature reviews neuroscience*, 13(6):407–420.

Casale, A. E., Foust, A. J., Bal, T., and McCormick, D. A. (2015). Cortical interneuron subtypes vary in their axonal action potential properties. *Journal of Neuroscience*, 35(47):15555–15567.

Chapko, R. and Kügler, P. (2004). A comparison of the Landweber method and the gauss–newton method for an inverse parabolic boundary value problem. *Journal of computational and applied mathematics*, 169(1):183–196.

Cox, S. and Wagner, A. (2004). Lateral overdetermination of the FitzHugh–Nagumo system. *Inverse Problems*, 20(5):1639.

Cox, S. J. and Griffith, B. E. (2001). Recovering quasi-active properties of dendritic neurons from dual potential recordings. *Journal of computational neuroscience*, 11(2):95–110.

Cox, S. J. and Ji, L. (2001). Discerning ionic currents and their kinetics from input impedance data. *Bulletin of mathematical biology*, 63(5):909–932.

Csercsik, D., Hangos, K. M., and Szederkényi, G. (2012). Identifiability analysis and parameter estimation of a single Hodgkin–Huxley type voltage dependent ion channel under voltage step measurement conditions. *Neurocomputing*, 77(1):178–188.

Daly, A. C., Gavaghan, D. J., Holmes, C., and Cooper, J. (2015). Hodgkin–Huxley revisited: reparametrization and identifiability analysis of the classic action potential model with approximate bayesian methods. *Royal Society open science*, 2(12):150499.

Ermentrout, G. B. and Terman, D. H. (2010). *Mathematical foundations of neuroscience*, volume 35. Springer Science & Business Media.

FitzHugh, R. (1961). Impulses and physiological states in theoretical models of nerve membrane. *Biophysical journal*, 1(6):445–466.

Grinvald, A. and Hildesheim, R. (2004). VSDI: a new era in functional imaging of cortical dynamics. *Nature Reviews Neuroscience*, 5(11):874–885.

Hadamard, J. (2014). *Lectures on Cauchy's problem in linear partial differential equations*. Courier Corporation.

Hanke, M., Neubauer, A., and Scherzer, O. (1995). A convergence analysis of the Landweber iteration for nonlinear ill-posed problems. *Numerische Mathematik*, 72(1):21–37.

He, Y. and Keyes, D. E. (2007). Reconstructing parameters of the FitzHugh–Nagumo system from boundary potential measurements. *Journal of Computational Neuroscience*, 23(2):251–264.

Hodgkin, A. L. and Huxley, A. F. (1952). A quantitative description of membrane current and its application to conduction and excitation in nerve. *The Journal of physiology*, 117(4):500–544.

Izhikevich, E. M. (2007). *Dynamical systems in neuroscience*. MIT press.

Kaltenbacher, B., Neubauer, A., and Scherzer, O. (2008). *Iterative regularization methods for nonlinear ill-posed problems*, volume 6. Walter de Gruyter.

Krinskiĭ, V. and Kokoz, I. M. (1973). Analysis of the equations of excitable membranes.I. reduction of the Hodgkins-Huxley equations to a 2d order system. *Biofizika*, 18(3):506–511.

Liley, D. T., Cadusch, P. J., and Dafilis, M. P. (2001). A spatially continuous mean field theory of electrocortical activity. *Network: Computation in Neural Systems*, 13(1):67.

Morris, C. and Lecar, H. (1981). Voltage oscillations in the barnacle giant muscle fiber. *Biophysical journal*, 35(1):193–213.

Nayak, A. (2021). Smoothing $\mathcal{L}^2$ gradients in iterative regularization.

Neubauer, A. (2000). On Landweber iteration for nonlinear ill-posed problems in Hilbert scales. *Numerische Mathematik*, 85(2):309–328.

Neubauer, A. (2018). A new gradient method for ill-posed problems. *Numerical Functional Analysis and Optimization*, 39(6):737–762.

Tadi, M., Klibanov, M. V., and Cai, W. (2002). An inversion method for parabolic equations based on quasireversibility. *Computers & Mathematics with Applications*, 43(8):927–941.

Valle, J. A. M. (2020). Predicting the number of total COVID-19 cases and deaths in brazil by the gompertz model. *Nonlinear Dynamics*, 102(4):2951–2957.

Valle, J. A. M., Madureira, A. L., and Leitão, A. (2020). A computational approach for the inverse problem of neuronal conductances determination. *Journal of Computational Neuroscience*, pages 1–17.

Walch, O. J. and Eisenberg, M. C. (2016). Parameter identifiability and identifiable combinations in generalized Hodgkin–Huxley models. *Neurocomputing*, 199:137–143.

Wang, G. J. and Beaumont, J. (2004). Parameter estimation of the Hodgkin–Huxley gating model: an inversion procedure. *SIAM Journal on Applied Mathematics*, 64(4):1249–1267.

Willms, A. R., Baro, D. J., Harris-Warrick, R. M., and Guckenheimer, J. (1999). An improved parameter estimation method for Hodgkin-Huxley models. *Journal of Computational Neuroscience*, 6(2):145–168.

DEPARTAMENTO DE MODELAGEM COMPUTACIONAL, LABORATÓRIO NACIONAL DE COMPUTAÇÃO CIENTÍFICA, AV. GETÚLIO VARGAS 333, 25651-070 PETRÓPOLIS, RJ, BRAZIL

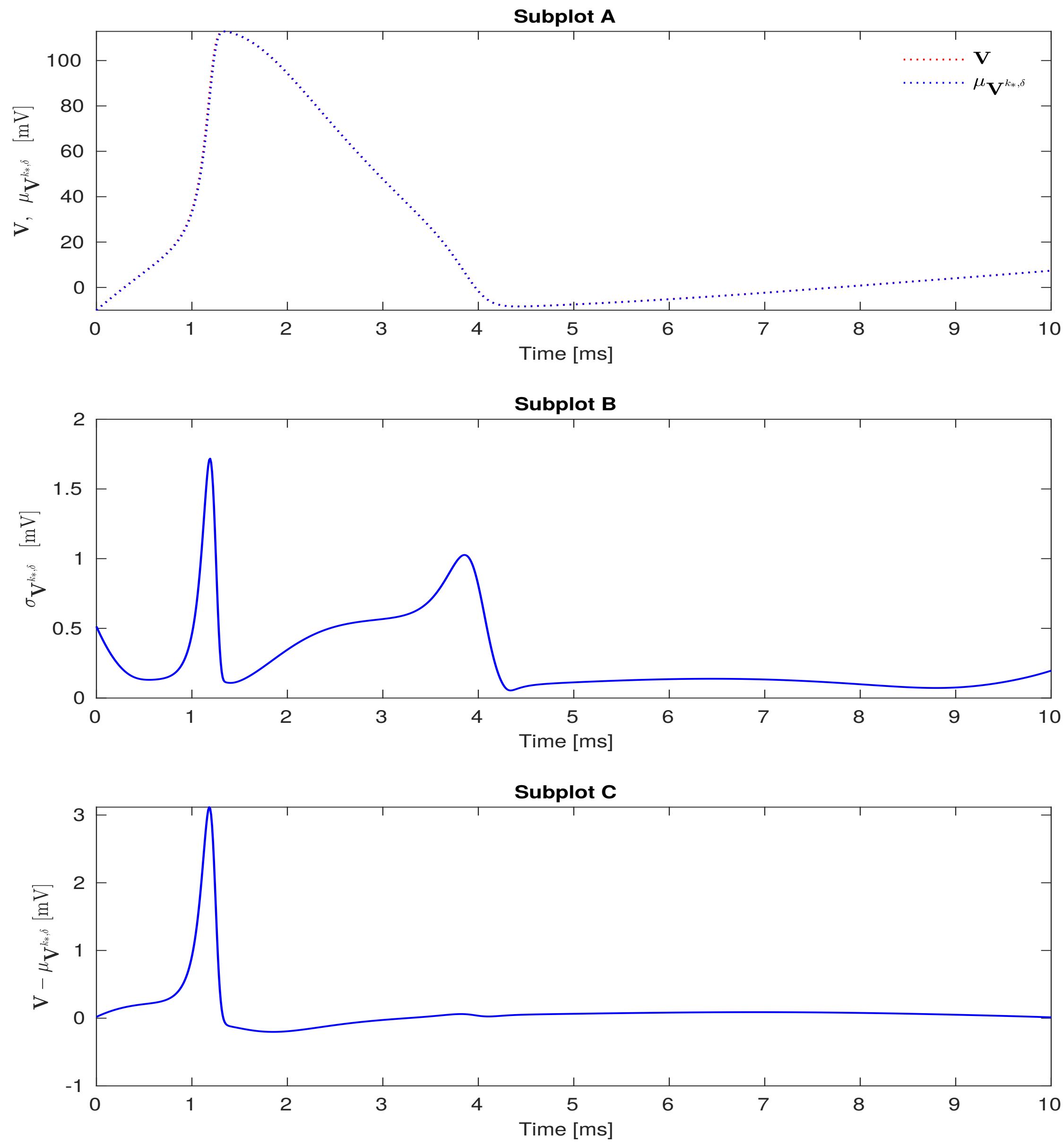

FIGURE 1. Results for Example 3.1 with $\varepsilon = 10\%$ and $M = 400$ experiments. In subplot A, the red line represents the exact membrane potential ($\boldsymbol{V}$), and the blue line is the mean of the approximations of the membrane potential obtained by the proposed method ($\mu_{\boldsymbol{V}^{k_*,\varepsilon}}$). Subplot B shows the standard deviation of the approximations of the membrane potential obtained by the minimal error method. Finally, Subplot C displays the difference between $\boldsymbol{V}$ and $\mu_{\boldsymbol{V}^{k_*,\varepsilon}}$.

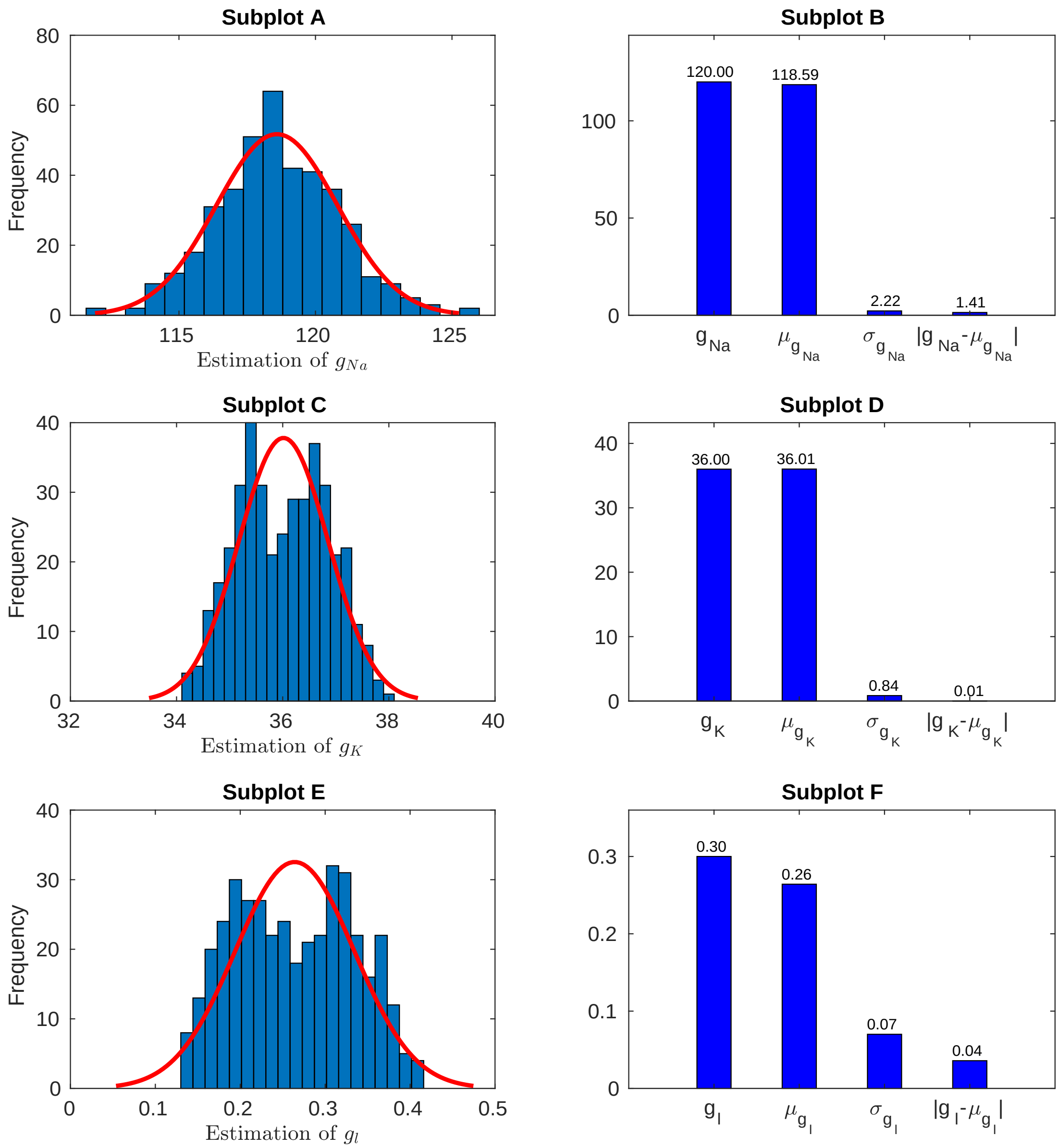

FIGURE 2. Results for Example 3.1 with $\varepsilon = 10\%$ and $M = 400$ experiments. Figures A-B, C-D, E-F show the maximum conductances of sodium, potassium and leakage. Histograms A, C and E show estimates for $g_{\text{Na}} = 120$, $g_{\text{K}} = 36$ and $g_l = 0.3$, with 400 experiments. The red line shows an "approximate" Gaussian. In Subplots B, D, F, the bars describe the exact maximum conductance, the mean of the estimated conductances, the standard deviation of the estimated conductances, and the absolute value of the difference between the exact maximum conductance and the mean of its estimates.

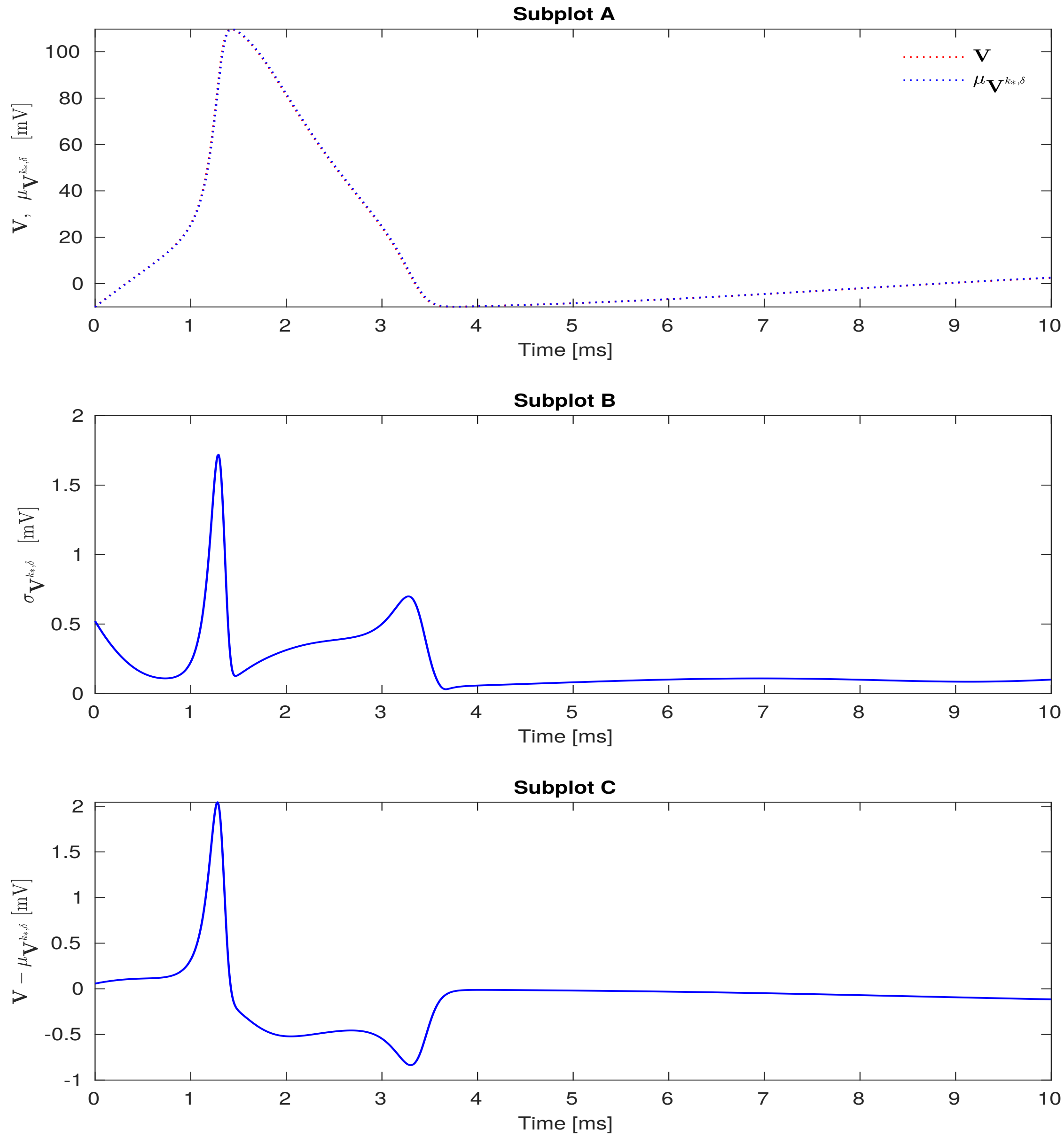

FIGURE 3. Results for Example 3.2 with $\varepsilon = 10\%$ and $M = 400$ experiments. See Figure 1 for the subplots description.

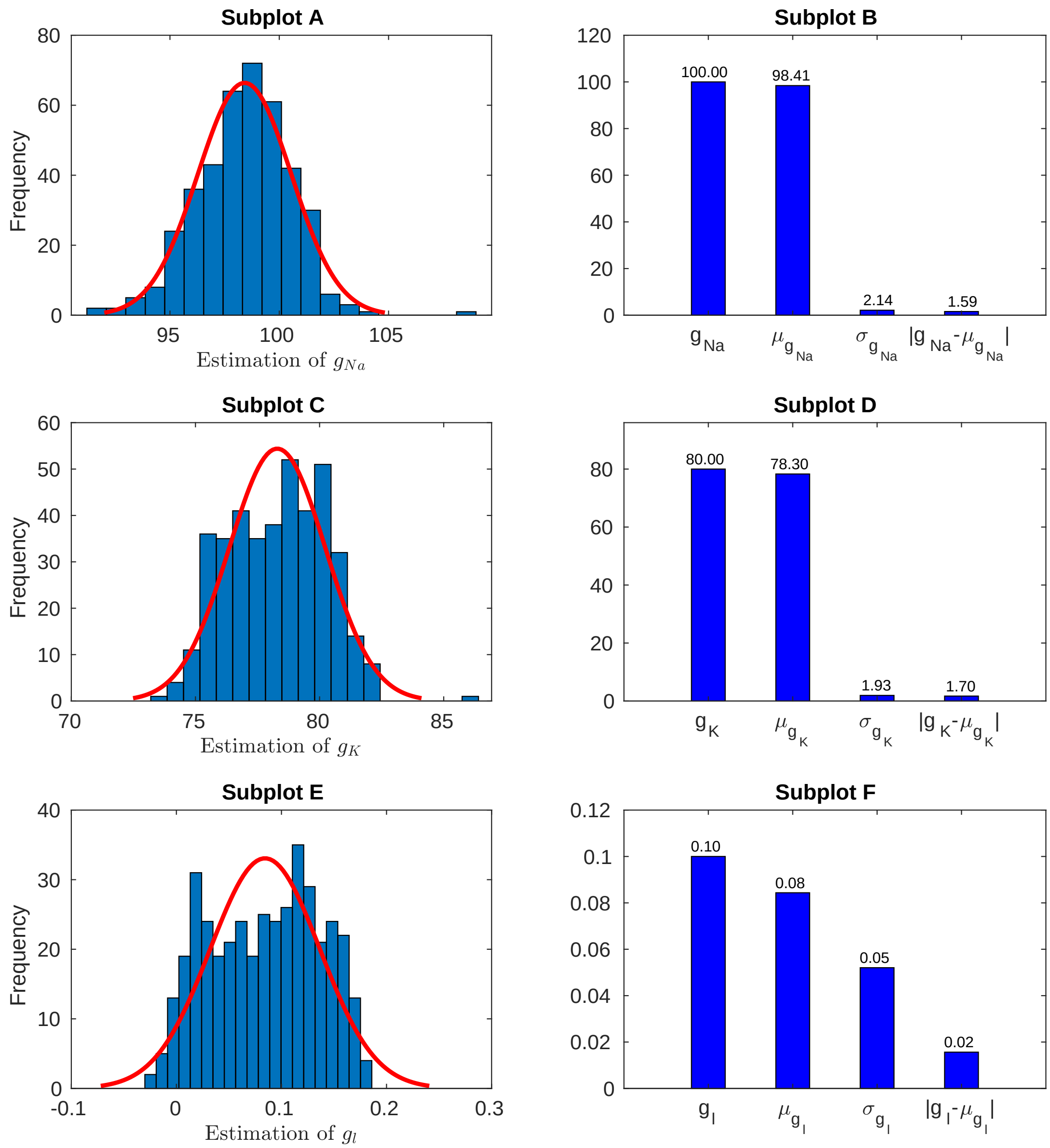

FIGURE 4. Results for Example 3.2 with $\varepsilon = 10\%$ and $M = 400$ experiments. The figure shows the statistical results when estimating $g_{\text{Na}} = 100$, $g_{\text{K}} = 80$ and $g_l = 0.1$. See Figure 2 for the Subplots description.

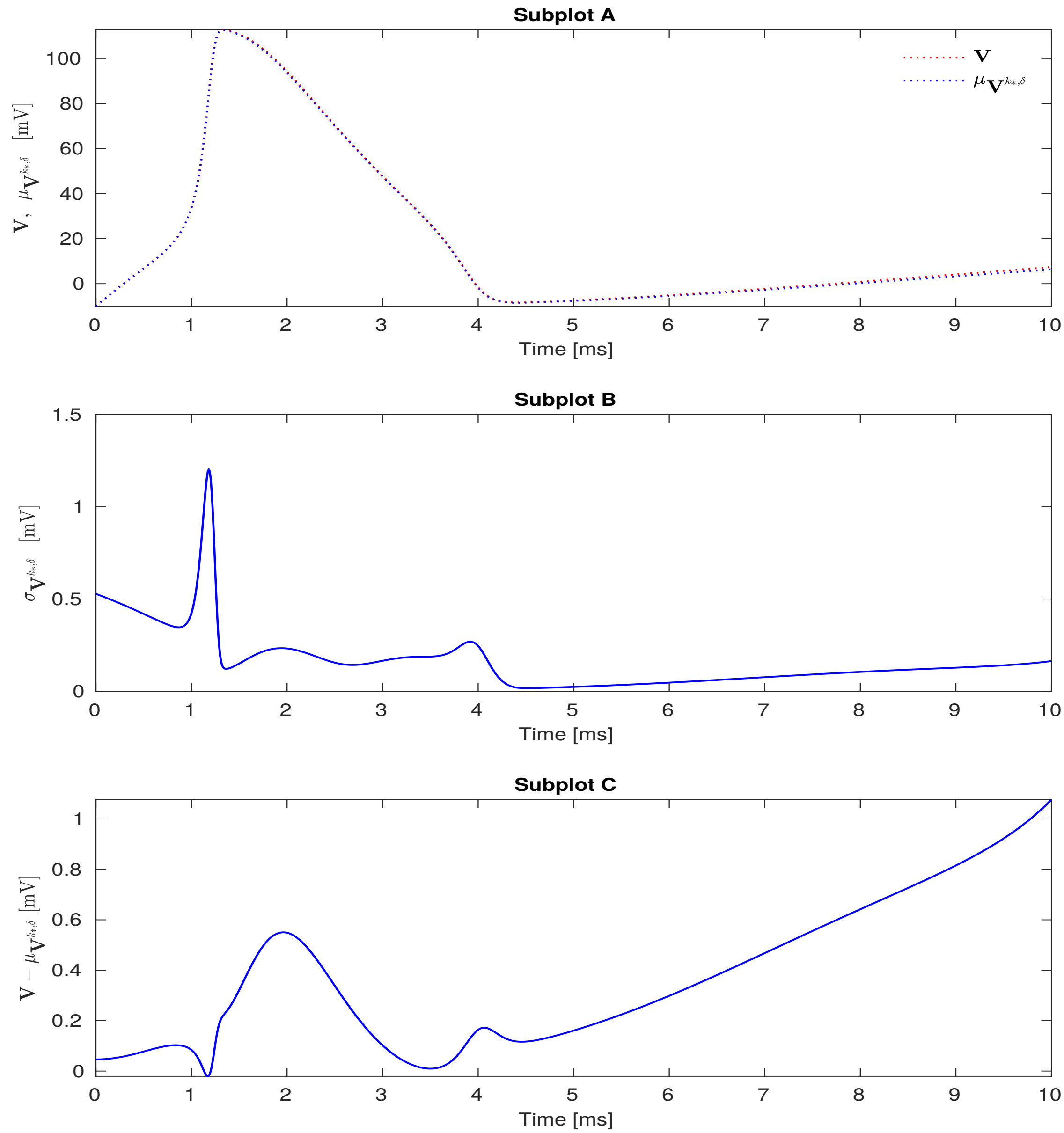

FIGURE 5. Results for Example 3.3 with $\varepsilon = 10\%$ and $M = 400$ experiments. See Figure 1 for the subplots description.

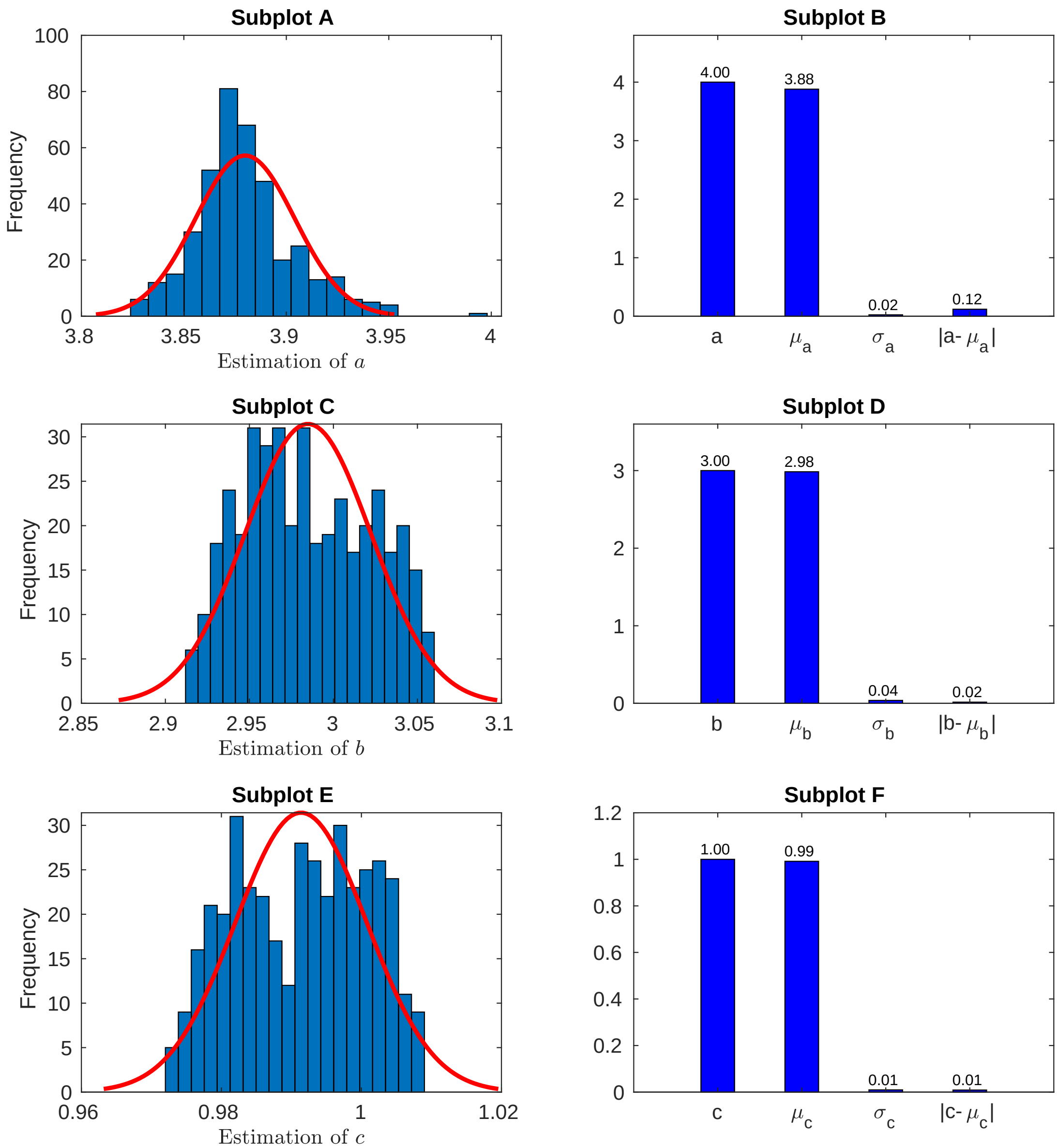

FIGURE 6. Results for Example 3.3 with $\varepsilon = 10\%$ and $M = 400$ experiments. This figure presents the statistical results when estimating $a = 4$, $b = 3$ and $c = 1$. See Figure 2 for the subplots descriptions.

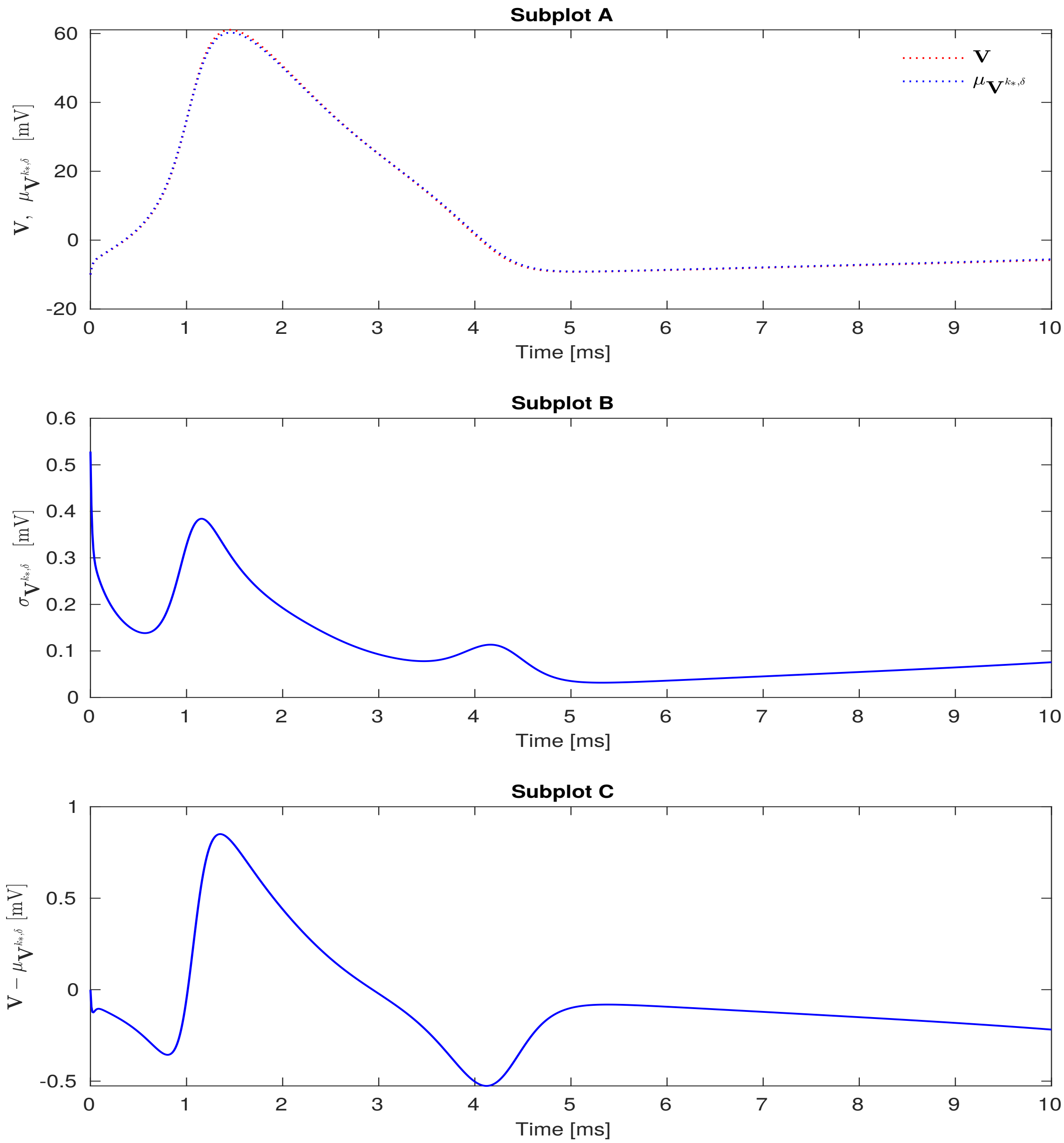

FIGURE 7. For Example 3.4 with $\varepsilon = 10\%$ and $M = 400$ experiments. See Figure 1 for the subplots description.

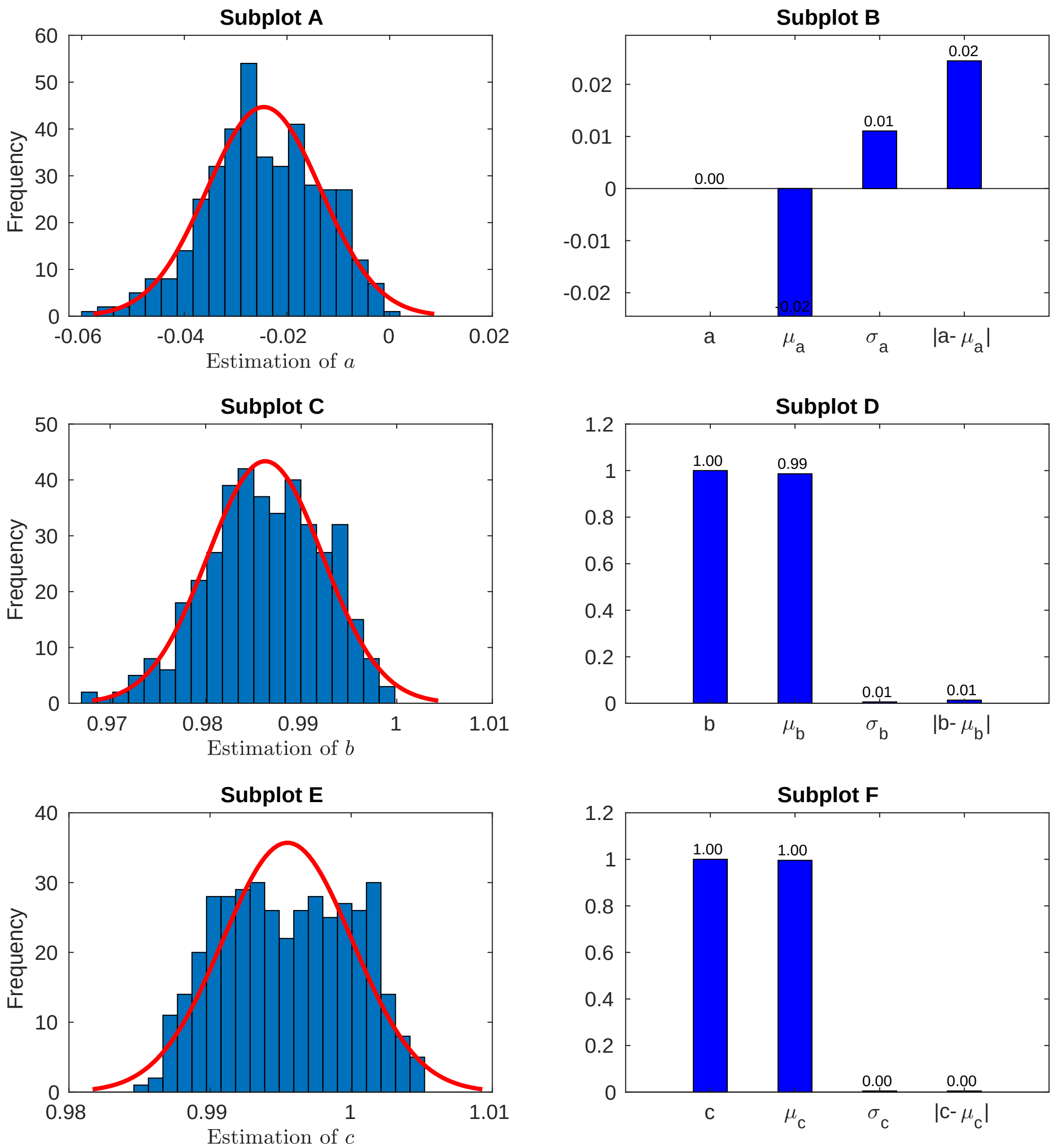

FIGURE 8. For Example 3.4 with $\varepsilon = 10\%$ and $M = 400$ experiments. The figure displays the statistical results when estimating $a = 0$, $b = 1$ and $c = 1$. See Figure 2 for the subplots descriptions.